university of groningen / faculty of science and engineering

Ocean Grazer

Integration Project IEM

On the scaling effects of a single-piston pump

Jaap Jonker

Bachelor Integration Project performed at The Ocean Grazer Project

4 July 2018

First supervisor: A.I. Vakis
Second supervisor: G.K.H. Larsen

University of Groningen
Faculty of Science and Engineering
Industrial Engineering and Management programme

Abstract

The Ocean Grazer is a device that converts wave energy into electricity. It uses a piston pump system that is driven by floaters, which move up and down with the motion of the waves. An experimental setup of this pumping system is developed at the University of Groningen, which is denoted as the Single-Piston Pump (SPP) prototype.

In order to understand the behaviour and efficiency of the SPP prototype, a mathematical simulation model has been designed by R.M. Zaharia, which addresses most of the characteristics of the SPP. One of the intended functions of this SPP model was, that it could determine how the SPP system behaves when it is scaled up to the full-scale size of the Ocean Grazer. However, due to the inherent nature of a distorted model, bias occurs when outputs of the SPP model are scaled straightforwardly with the Froude law. Therefore, one of the goals of this research is to the check whether the SPP model, with correctly scaled initial parameters, is valid to determine the efficiency of the full-scale model. Another aim of this research is to evaluate the scaling effects of factors that are not taken into consideration in the SPP model, but will be of influence on the outputs.

The SPP model with adjusted initial parameters is enlarged with different scaling ratios. Outputs such as, forces, energies and efficiencies are analysed to determine the validity of the model. Furthermore, the forces and energies, regarding the SPP prototype in its initial size, are scaled up straightforwardly to compare the theoretical values with the ones determined by the SPP model.

Table of contents

1. Introduction

1.1 Renewable Energy

Currently, most of the world still relies on coal, oil, nuclear energy and natural gas for its energy supply [1]. All four of these energy sources are non-renewable and their quantity is not infinite either which eventually results in their extinction. Furthermore, the contribution of non-renewable energy source on global warming and climate change becomes more self-evident . Since the effects on the environment are making themselves increasingly felt and cannot be ignored anymore, the urge for environmental friendly solutions becomes more dominant. The most common solution for this problem, is the use of renewable energy sources. They produce little to no global warming emissions and their source is infinite. The total energy production of renewable energy sources is still very small compared to the traditional non-renewable fuels, however, their development is an ongoing process with the end of it not yet in sight.

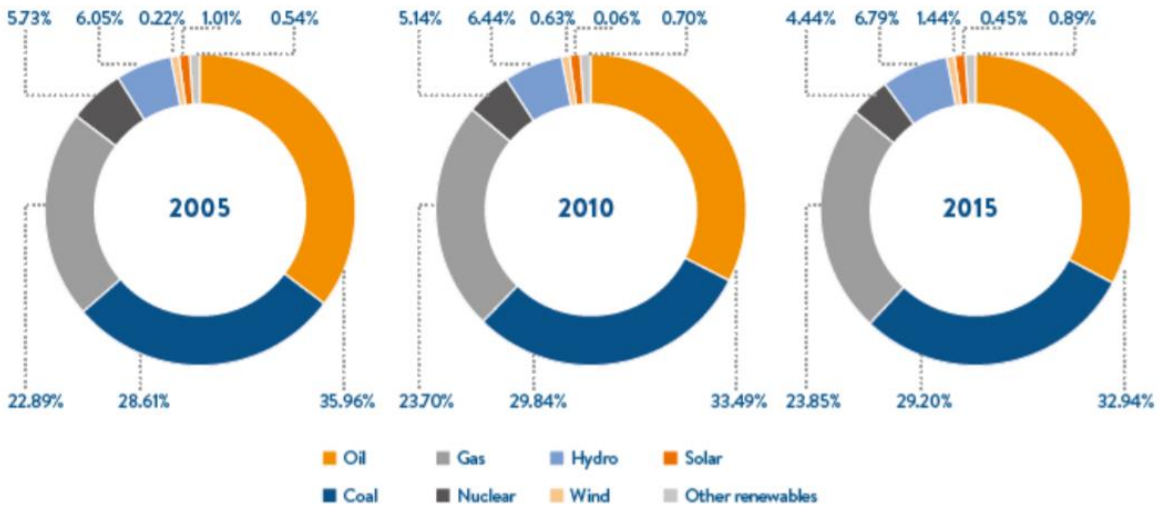

Figure 1: Primary energy consumption over the past 15 years [2].

Within the European Union each individual European country had its own available resources and their own unique energy market. Due to the uniqueness of the availabilities, each European country has their own specific plan to meet their targets for renewable energy [3]. Furthermore the European countries have agreed on new EU-wide climate and energy targets.

Targets for 2030:

- a 40% cut in greenhouse gas emissions compared to 1990 levels
- at least a 27% share of renewable energy consumption
- at least 27% energy savings compared with the business-as-usual scenario.

These targets include an large increase in renewable energy, whereby the development of different renewable energy devices becomes even more important.

1.2 Renewable Energy Devices

Over the years multiple renewable energy devices have been developed [4]. Most of the renewable energy is captured from the sun by solar panels. The solar panels are used to transfer the captured energy from the sun, directly into electricity. Next to solar panels, wind turbines are becoming more common in the present day landscape and are responsible for a big part of the total renewable energy production. The wind turbine consists of blades which are connected to a turbine. When the wind blows past the blades, they start to rotate. This rotation is transferred into electricity using the turbine. The third common type is a heat exchanger, which uses the heat of the Earth itself to produce renewable energy. The inside of the Earth has a constant temperature that is used to warm or cool households using a heat exchanger and a pump. Furthermore, dams or rivers that have a constant flow of water use turbines driven by hydropower and thereby, generate electricity. Besides the more common renewable energy devices, there are also energy devices that use emerging renewable energy sources. One of those sources is marine energy, which uses the tides and waves of the ocean. There are multiple projects that try to capture energy from the tides and waves and most of them are still in development. One of those is the Ocean Grazer, which fulfils a central role in the remainder of this research.

1.3 The Ocean Grazer

The Ocean Grazer is a device that converts wave energy into electric energy [5] and will also be used as a platform for other renewable energy sources, such as wind turbines [6]. Due to the versatile energy sources of the Ocean Grazer, it shows great potential as being a successful project for the production of renewable energy. Currently, the Ocean Grazer research team, at the University of Groningen, is occupied with the further development of the project.

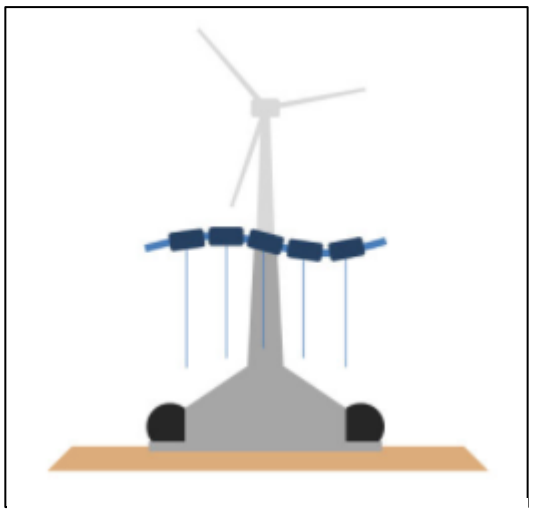

Figure 2: Schematic representation of the Ocean Grazer device

The main technology of the Ocean Grazer is the conversion of wave-energy into electric energy. Floaters move up and down with the amplitude of the waves. These floaters are connected to a piston pump which utilises the motion of the floaters to pump a working fluid from a lower section to an upper section. As a consequence, a pressure difference occurs. In the first phase of the Ocean Grazer, the device was designed to be a big floating platform. However, over the couple of years research showed that the idea of a floating platform was not feasible. Currently, the Ocean Grazer reached the third generation and is designed to be in the housing of a wind turbine. This wind turbine is surrounded by a bladder. As a result of the pressure difference, the working fluid flows in and out this bladder, with the outflow passing a turbine. This turbine converts the flow of the fluid into electric energy.

In order to understand the behaviour of the Ocean Grazer, multiple experimental setups have been developed. One of them is a scale size version of the pumping system, which is

used in combination with a mathematical simulation model to derive relevant outputs and predictions. The usefulness of the outputs and predictions are doubtful, since the scaling effects of enlarging the experimental setup to its intended size are unclear. In this research, the scaling effects of the pumping system will be investigated.

1.4 Technology Readiness Level

The Technology Readiness Level (TRL) application is a tool to determine the maturity of a new technology [7]. It can be used as a guideline for understanding the current situation of the projects, as well as a tool to identify the next steps in the development. Eventually, completing all the TRL levels, should result in technology adoption.

The Ocean Grazer has been going through three concepts, where the first two were considered as not feasible. The third and current concept is less colossal and financial more attractive, however, the fundamental technology of the pumping system has not changed. In terms of TRL level, the Ocean Grazer can be categorized in level 4. Two different experimental setups have been developed, one consist out of floaters driven by generated waves, whereas the second is a pumping system. A third experimental setup is in development, which consist of the bladder that should surround the wind turbine. All experimental setups are still in laboratory environment and are not interconnected, which locates it in TRL-level 4. Eventually, to reach TRL-level 9, the technology needs be proven in operational environment. Therefore, it is critical that the behaviour of a full-scale SPP can be predicted, so that possible errors can be prevented.

	TRL	Description
Basic Research	1	Basic principles and research
	2	Application formulated
	3	Proof of concept
Applied Research	4	Components validated in laboratory environment
	5	Integrated components demonstrated in a laboratory environment
Development	6	Prototype demonstrated in relevant environment
	7	Prototype demonstrated in operational environment
	8	Technology proven in operational environment
Implementation	9	Technology refined and adopted

Figure 3: Technology readiness levels

2. Problem Analysis

2.1 System Description

In this research, the focus is on the single-piston pump (SPP), which is a subsystem of the Ocean Grazer and is responsible for converting the movement of a floater into potential energy [5]. The floater is connected to the piston with a cable. The cable pulls the piston upwards when the waves lift the floater. When the pulling force of the floater is large enough the piston moves upwards in a cylinder. The motion of the piston, pumps a working fluid upwards. Simultaneously with the piston moving upwards, a check valve opens in the bottom of the cylinder as a result of vacuum force. When the check valve is open, the cylindrical space beneath the piston is filled with the working fluid. When the floater moves down again, the piston sinks because of its mass. Throughout the sinking of the piston, the piston valve itself opens, so that the cylindrical space above the piston is filled up again with the working fluid. This cycle repeats itself over and over again.

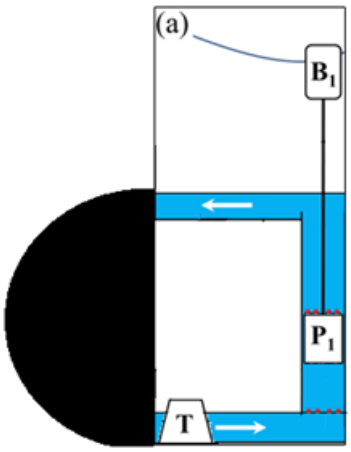

Figure 4: schematic representation of the single-piston pump

Due to the working fluid that is pumped upwards, a pressure difference occurs between the working fluid above and under the piston. The working fluid above the piston is under a higher pressure the working fluid below the piston. As a result of this higher pressure, the working fluid flows in a bladder, which is located around the outside of the structure of the wind turbine [6]. The bladder can be seen as a sort of tube and will be elastic. The elasticity of the bladder in combination with the pressure of the water column around the bladder lead to a force, acting on the working fluid inside the bladder. This working fluid has the availability to flow back from the bladder to the space beneath the piston. When the working fluid flows back, it passes a turbine, which converts the flow into electric energy.

The working principles of the single-piston pump are used to develop an experimental setup, which will be addressed as the SPP prototype [8]. The SPP prototype uses a motor that simulates the buoyancy force and drives the piston. The piston of the SPP prototype pumps the working fluid from a lower to an upper reservoir, and not into a bladder. The parameters and behavior of the SPP prototype are transferred to an mathematical simulation model (SPP model), which is used to calculate relevant outputs as forces, energies and efficiencies [8]. Since the SPP model has a dominant role during this research, the boundaries will be based on the prototype, where the input is the motion of the motor and the output is the working fluid stored in the upper reservoir.

2.2 Problem Statement

Currently the Ocean Grazer research team developed a prototype of the SPP which is about three meters tall. Mechanically simulated waves provide the motion for the piston to move. The movement of the piston is transferred in potential energy by means of a pressure

difference. Briefly worded, the prototype behaves as the intended full-scale SPP and provides much information and data on the behavior of the single-piston pump. In combination with the SPP model relevant outputs can be calculated and predicted. However, the prototype is about three meters tall, whereas the full sized single-piston pump will be, approximately, one hundred meters tall.

The problem that occurs for the Ocean Grazer research team is that it is unclear what the precise effects of scaling will be, which results in possible errors in outputs of the SPP model. Scaling up the measured forces straightforwardly results in a distorted picture due to the inherent nature of the prototype. In other words, the effects of scaling the SPP are unclear and therefore, the efficiency of a full-scale single-piston pump cannot be predicted.

This leads to the following problem statement:

"Scaling effects of a SPP are not taken into account properly, whereby it is impossible to give an accurate prediction of the efficiency of a full-scale SPP."

2.3 Problem Owner Analysis

Within this research, two problem owners are available. The first one is M. van Rooij, he has an interest in this research as project leader and creator of the first experimental prototype. As project leader he is concerned with the commercial side of the Ocean Grazer and valid models are very useful in proving the potential of the Ocean Grazer to investors. Second, as the leader of the Ocean Grazer research team, A.I. Vakis is concerned with the ongoing development of all parts in the Ocean Grazer project. Research on the scaling effects of the SPP is important for the development of the Ocean Grazer project, because it will determine the validity of the SPP model. Therefore, A.I. Vakis has an interest in the outcome of this research.

2.4 Stakeholder Analysis

In this case the stakeholders are the same persons as the problem owners. The first stakeholder is M. van Rooij, as project leader and creator of the experimental prototype, he would benefit from optimizing the mathematical model. As project leader, it is also important to raise money for further development of the project. Therefore, it is necessary to convince investors to invest in the project. To do so, it is important that the predictions presented to the sponsors will hold when the experimental prototype is scaled. The second stakeholder is A.I. Vakis, leader of the Ocean Grazer research team. As a leader he has a stake in this research since investigating and improving the SPP model would definitely help with the prediction of the full-scale efficiency, which is beneficial for the overall development. Furthermore, it is important to mention that both stakeholders do not have a conflict and both of them pursuit the same goal.

2.5 Research Goal

As described in the problem statement, the scaling effects are not taking into account properly and therefore, it is impossible to give an accurate prediction of the efficiency of a

full-scale single-piston pump. Therefore, the SPP model needs to be adjusted in order to scale the SPP correctly. The goal of this research can therefore, be stated as:

"To evaluate the scaling effects of the adjusted SPP model and predict the efficiency of a full-scale single-piston pump."

To fulfill this goal, first, all of the relevant parameters in the mathematical simulation model need to be determined. Second the parameters need to be scaled correctly. Finally, the mathematical simulation model needs to be tested to check whether the outputs are valid.

2.6 Research Question

Considering the problem definition and the research goal, three sub research question can be derived. The sub research questions are:

1. "Which scaling law is appropriate for scaling the SPP?"

2. "How can the parameters in the SPP model be adjusted taking the scaling in consideration?"

3. "How are the results of the SPP model influenced by different scaling?"

Combining the sub research questions result in one overall research question. This research question is phrased as follows:

"How is the predicted efficiency of the adjusted SPP model affected by the scaling effects?"

3. Research Design

3.1 Research Methodology

The main method that is used throughout this research is the OBS-method [10], which is explained during the course "Business System Design" given by Drs. W.A. Prins at the University of Groningen. The OBS-method is an variation on the Regulative Cycle of van Strien [11]. Furthermore, it utilizes a particular system thinking based on the ideas of Jackson [12], where the OBS-method covers both the functionalist as the interpretive paradigm.

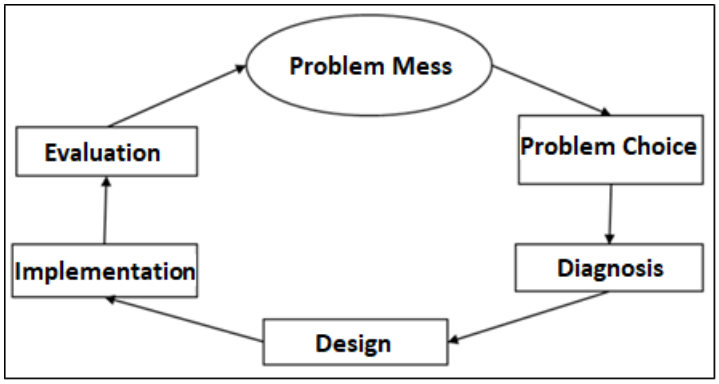

Figure 5: Regulative cycle

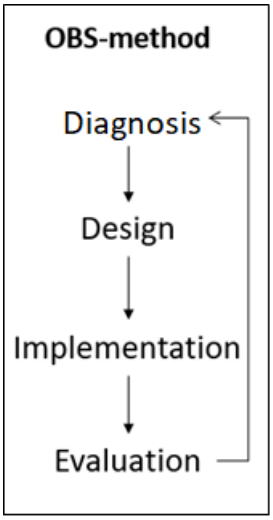

Figure 6:OBS-method

The OBS-method can be seen as an iterative cycle in which every step is an iterative cycle on its own. The first phase is to diagnose the problem, which covers the problem mess, problem choice and diagnosis in the Regulative cycle of van Strien in figure 3. The diagnosis phase consists of the following steps:

<u>Problem/Goal determining phase</u>

- Context
- Problem owner analysis
- (First) system description and analysis
- Stakeholder analysis
- Problem definition & goal of the research

<u>Conceptual research design</u>

- Formulate main research question(s)
- Literature study
- Create conceptual causal model
- Formulate sub-questions
- Operationalization of concepts
- Choice of tools and techniques
- Data gathering plan

Empirical diagnosis

- Execution of data gathering
- Data-analysis
- Answering sub research questions
- Create the empirical causal model

After the diagnose phase is finished, the design phase is encountered. The design phase covers the following steps:

Design

- Judgement on empirical causal model
- Formulate design question(s)
- (Re)design system
- Choice of (re)design (when needed)
- Evaluate (re-design)

The third and fourth phase in the OBS-method are implementation and evaluation, which are the same as the last two phases of the Regulative cycle. Furthermore, the whole cycle starts again if the results of the evaluation are not satisfactory.

3.2 Data Acquisition

All of the data was derived from the SPP model, which consist out of MATLAB-scripts and a Simulink-model. The MATLAB-scripts provided all of the parameters and calculations that influenced the outcome of the Simulink-model. These were the parameters that needed to be investigated on how they scale in order to determine how they influence the model. The Simulink-model provided a clear overview of which parameter is connected to which physical block of the SPP and could be adjusted where necessary. Furthermore, literature was used to provide an more analytical view on the SPP, rather than focussing strictly on the values and dimensions of the parameters.

3.3 Literature Resources

Most of the literature used throughout the research is existing out of books and articles. At first instance, articles from the Ocean Grazer website are used to acquire the knowledge about the fundamentals of the SPP. Furthermore, articles and relevant documents are supplied by Y. Wei, PhD student and member of the Ocean Grazer research team. In addition, two databases, SmartCat and Google Scholar, are used for books and articles necessary for information that is not already available. They are use primarily for the collection of decent scaling laws.

First search terms that were used are:

- Scaling laws
- Similarity laws
- Fluid dynamics
- Scaling flows

3.4 Risk Analysis

A risk analysis was conducted to act against the risks that have the potential to be responsible for failure of this research. First, it was important to identify the possible threads that could play a role in the outcome of the research. After the threads were identified, it was necessary to determine the risk they carried with them. When the risks were determined, they should be parried in a decent way. A schematic overview of the risk analysis is stated below.

Table 1: Risk analysis

Thread	Risk	Risk Management
Quality	The scaling effects of the MATLAB/Simulink-model are not determined properly, causing future mistakes in the Ocean Grazer development.	Within the development of the SPP, it is critical that nothing is overlooked. A clear research question and design goal will avoid this.
Time	The timeframe set for the research is short and, therefore, has a high risk of not meeting the deadline and delaying the whole project	A well thought planning with realistic deadlines will give the support needed to achieve the desired goal in time.
Knowledge	This research requires a sufficient amount of knowledge that has to be acquired throughout the project, to achieve the desired goal. The risk is, that the knowledge acquired is not sufficient.	The right supervision and motivation will lead to self-education. Acquiring the knowledge needed for the development of the SPP model is one the steps within this self-education.

3.5 Tools and Techniques

Within this research, multiple tools and techniques were used to determine the effects of scaling on the efficiency of a full-scale SPP. The tools and techniques can be classified as physical laws, mathematical modelling and simulation modelling.

The first tool that was used is the conceptual model, it gives a clear overview of the fundamentals of the SPP. The main components are interconnected and indicate the relationship between them. Although the conceptual model is very simplistic, it was very useful in understanding the model during the first steps of this research.

Secondly, a numerical computing software called MATLAB, was used for mathematical modelling. MATLAB was used by R. Zaharia to develop a script that represents the dimension and behaviour of the SPP prototype [9]. The MATLAB-script was used in combination with a Simulink model. Simulink is a simulation software that uses physical blocks to represent the lay-

out of the model. The different physical blocks are assigned with a value or function by the MATLAB-script.

At last, to acquire knowledge on scaling of the experimental SPP, scaling laws were used. The scaling laws will define the impact of scaling on each component, factor or constant in the MATLAB-script.

3.6 Conceptual Model

To obtain better understanding of the SPP, a very simplistic conceptual model has been designed. It shows the fundamentals of the SPP in an overview. The plus and minus sign represent the increase or decrease, the close and open concern the functionality of the valves, the up and down are related to the displacement of the piston, and the spring/damper is an indication of the working properties of the cable between floater and piston.

Conceptual model explained:

- Up movement of the piston results in: piston valves close, check valves open, volume above the piston decreases, volume below piston increases and a increase in potential energy.
- Down movement of the piston results in: piston valves open, check valves close, volume above the piston increases and volume below the piston decreases.

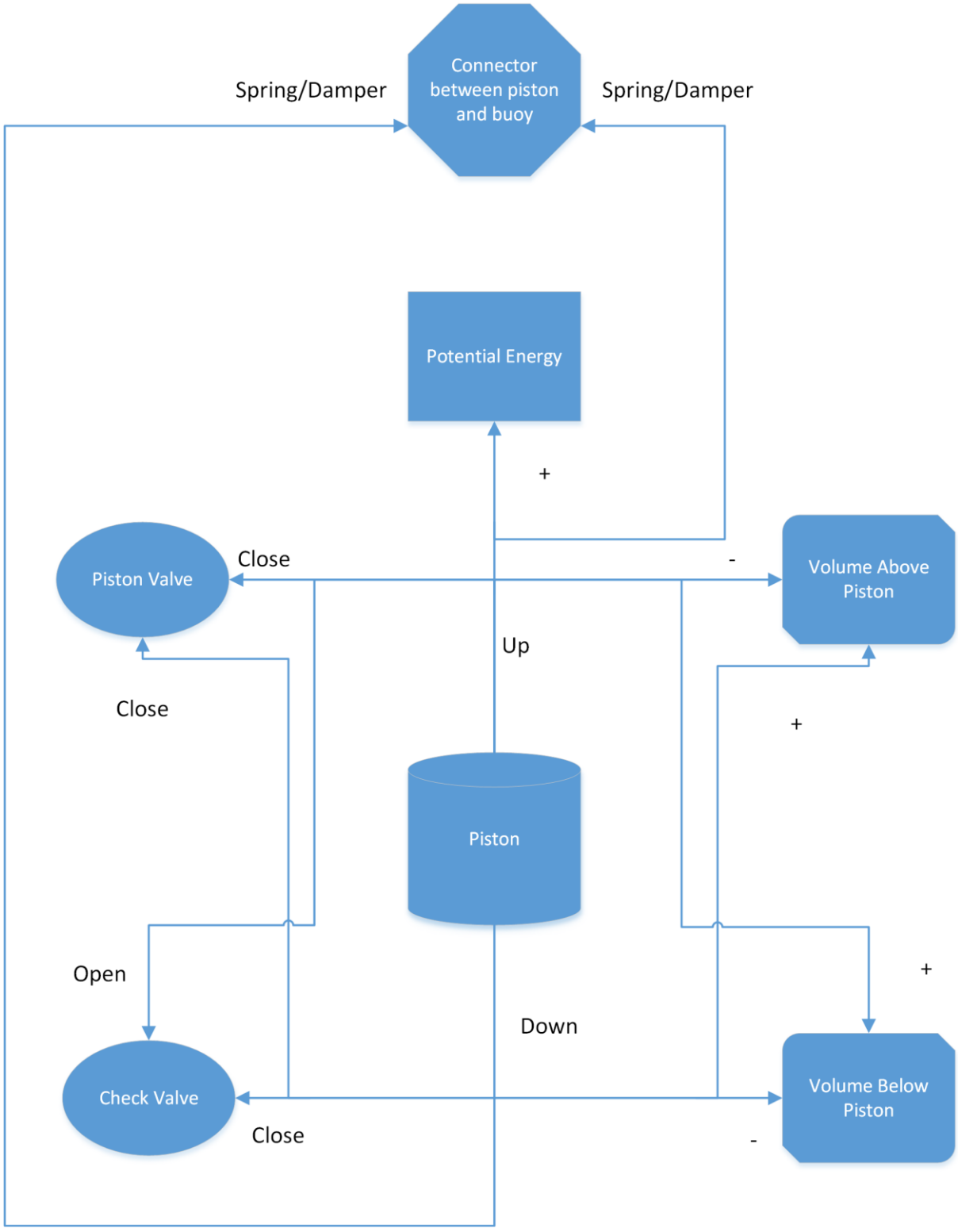

Figure 7: Conceptual model

4. Scaling Laws

4.1 The Froude Number

In the scaling of the SPP the phenomenon of geometric similarity is used to determine the lengths of the different parameters [13]. If the physical length of the prototype is denoted by (L_p) and the length of the model by (L_m), than the length ratio (L_r) is calculated by,

$$L_r = \frac{L_m}{L_p}. \tag{1}$$

This only holds if the length scale of the prototype and its models are taken as constant, and therefore, are geometrically similar.

Velocity can also be used to determine a ratio between the prototype and the model, using kinematic similarity,

$$V_r = \frac{V_m}{V_p}, \tag{2}$$

where (V_m) is the velocity of the model, (V_p) the velocity of the prototype and (V_r) is than velocity ratio. The velocity is based on the distance travelled over time and therefore,

$$V_m = \frac{L_m}{T_m}, \tag{3}$$

$$V_p = \frac{L_p}{T_p}, \tag{4}$$

$$V_r = \frac{\frac{L_m}{T_m}}{\frac{L_p}{T_p}} = \frac{L_m}{T_m}\frac{T_p}{L_p} = \frac{L_m}{L_p}\frac{T_p}{T_m} = \frac{L_r}{T_r}, \tag{5}$$

where (T_r) is the time ratio between the time of the model (T_m) and the prototype (T_p), and is stated as,

$$T_r = \frac{T_m}{T_p} \tag{6}$$

Furthermore, the acceleration scale can be derived in a similar way,

$$a_m = \frac{V_m}{T_m} = \frac{V_r\, V_p}{T_r\, T_p} = a_r\, a_p, \tag{7}$$

$$a_r = \frac{a_m}{a_p} = \frac{V_r}{T_r} = \frac{L_r}{T_r^2}, \tag{8}$$

with (a_m) representing the acceleration of the model, (a_p) the acceleration of the prototype and (a_r) the ratio between them. The Froude models use the characteristics of the

gravitational force with respect to a reference force, which is the inertia force. The inertia force is based on the 2nd law of Newton and is stated by,

$$F_{ine} = m\, a, \tag{9}$$

where (F_{ine}) is the inertia force, (m) is the mass and (a) is the acceleration. Furthermore, (m) and (a) can be defined as,

$$m = \rho\, L^3 \tag{10}$$

and

$$a = \frac{L}{T^2}. \tag{11}$$

Denoting (ρ) as the density and (L) as the length. Next, the gravitational force is defined as,

$$F_{gr} = m\, g, \tag{12}$$

where (m) is the mass and (g) is the gravitational acceleration. The mass (m) is defined in the same way as in equation (10). The ratio between the inertia force and the gravitational forces can be written as,

$$\frac{(F_{gr})_m}{(F_{ine})_m} = \frac{(F_{gr})_p}{(F_{ine})_p}, \tag{13}$$

which consequently is,

$$\frac{\rho_m\, g\, L_m^3}{\rho_m\, L_m^3\, \frac{L_m}{T_m^2}} = \frac{\rho_p\, g\, L_p^3}{\rho_p\, L_p^3\, \frac{L_p}{T_p^2}}, \tag{14}$$

resulting in,

$$\frac{g\, T_m^2}{L_m} = \frac{g\, T_p^2}{L_p}. \tag{15}$$

The time (T^2) in equation (15) can be defined as $T = \frac{L}{V}$, since $V = \frac{L}{T}$. As a consequence, equation (15) will be defined as,

$$\frac{g\, L_m^2}{V_m^2\, L_m} = \frac{g\, L_p^2}{V_p^2\, L_p}. \tag{16}$$

The inverse of this equation is,

$$\frac{V_m^2}{g\, L_m} = \frac{V_p^2}{g\, L_p}, \tag{17}$$

which results in the Froude number (Fr),

$$F_r = \frac{V}{\sqrt{g\,L}}. \tag{18}$$

Equation (17) states that the Froude number of both the prototype as the model, at a point, should be the same. The usage of Froude models result in the following Froude scaling table,

Table 2: Froude scaling table

Parameter	Unit	Multiplication factor
Length	[m]	L_r
Area	[m²]	L_r^2
Mass	[Kg]	L_r^3
Moment	[Nm]	L_r^4
Time	[s]	$\sqrt{L_r}$
Velocity	[m/s]	$\sqrt{L_r}$
Pressure	[Pa=N/m²]	$\rho_r\, L_r$
Discharge	[m³/s]	$L_r^{5/2}$
Force	[N]	$\rho_r\, L_r^3$
Energy	[J]	L_r^4

4.2 The Reynolds Number

The Reynolds number is based on the same similarity equations as the Froude number and therefore, equation (1) till equation (11) will hold for both numbers. The Reynolds number also uses the inertia force (F_{ine}) as reference force, but with respect to the viscosity force (F_{vis}). The viscosity force can be defined as,

$$F_{vis} = \tau\, A, \tag{19}$$

where (τ) is the shearing stress and (A) is the area. The shearing stress can also be defined as,

$$\tau = \mu\, \frac{du}{dy}, \tag{20}$$

with (μ) denoting the viscosity.

Therefore,

$$F_{vis} = \mu\, \frac{du}{dy}\, A. \tag{21}$$

The viscosity force defined in its dimensions $[F_{vis}]$ is stated as,

$$[F_{vis}] = \mu\, \frac{[LT^{-1}]}{[L]}\, [L^2]. \tag{22}$$

Furthermore, the equality ratio between the inertia force and the viscosity force is stated as,

$$\frac{(F_{vis})_m}{(F_{ine})_m} = \frac{(F_{vis})_p}{(F_{ine})_p}, \tag{23}$$

$$\frac{\mu_m \left(\frac{L_m T_m^{-1}}{L_m}\right) L_m^2}{\rho_m L_m^3 \left(L_m T_m^{-2}\right)} = \frac{\mu_p \left(\frac{L_p T_p^{-1}}{L_p}\right) L_p^2}{\rho_p L_p^3 \left(L_p T_p^{-2}\right)}. \tag{24}$$

Equation (24) can be rewritten, after cancellations, as,

$$\frac{\mu_m T_m}{\rho_m L_m^2} = \frac{\mu_p T_p}{\rho_p L_p^2}. \tag{25}$$

The time (T) in equation (25) can be defined as $T = \frac{L}{V}$, since $V = \frac{L}{T}$. As a consequence, equation (25) will be defined as,

$$\frac{\mu_m L_m}{\rho_m L_m^2 V_m} = \frac{\mu_p L_p}{\rho_p L_p^2 V_p}. \tag{26}$$

The inverse of this equation is,

$$\frac{\rho_m V_m L_m}{\mu_m} = \frac{\rho_p V_p L_p}{\mu_p}, \tag{27}$$

which results in the Reynolds number (Re),

$$Re = \frac{\rho V L}{\mu}. \tag{28}$$

Equation (27) states that the Reynolds number of both the prototype as the model, at a point, should be the same. The usage of Reynolds models result in the following Reynolds scaling table,

Table 3: Reynolds scaling table

Parameter	Unit	Multiplication factor
Length	[m]	L_r
Area	[m²]	L_r^2
Mass	[Kg]	L_r^3
Moment	[Nm]	L_r^4
Time	[s]	$L_r^2 \frac{\rho_r}{\mu_r}$
Velocity	[m/s]	$\frac{1}{L_r} \frac{\mu_r}{\rho_r}$
Pressure	[Pa=N/m²]	$\frac{\mu_r^2}{\rho_r} \frac{1}{L_r^2}$
Discharge	[m³/s]	$L_r \frac{\mu_r}{\rho_r}$
Force	[N]	$\frac{\mu_r^2}{\rho_r}$
Energy	[J]	L_r

4.3 Froude Models vs. Reynolds Models in the case of the SPP

Both the Froude and Reynolds numbers imply that,

$$Fr_m = Fr_p \tag{29}$$

and,

$$Re_m = Re_p \tag{30}$$

However, it is inconsistent to use both Froude as Reynolds similarity at the same time. Therefore, it is necessary to determine which of the two scaling models is the one most suitable for the SPP. To do so, both models are compared with the discharge. In the SPP, with upscaling, both the volume as the passage area increase. The volume increases with the length ratio to the power of three, whereas the passage area increases with the length ratio to the power of two. Consequently, the volume becomes bigger in comparison to the passage area and in one stroke the discharge will increase. The discharge is calculated with,

$$Q = V\,A, \tag{31}$$

where Q is the discharge (m^3/s), V is the velocity (m/s) and A is the passage area (m^2). Since both Froude as Reynolds imply that the area increases with the length ratio to the power of two, the difference will be in the discharge and the velocity. Reynolds states that the discharge increases linear, while the velocity decreases, which is only possible if the time, one stroke takes, increases quadratic. The SPP model show that this is not the case and that the time increases roughly with the square root of the length ratio, which is according to the scaling of Froude.

Furthermore, Reynolds states that the force increases with $\frac{\mu_r^2}{\rho_r}$, which means the piston force will not increases, since the viscosity and the density of the working fluid stays equal. The Simulink model shows that the piston force increases, even though the viscosity and density stay the same. This is another indication that Froude scaling is more suitable for the SPP.

Besides the discharge and the force, it is clear that gravity has an influence on the piston, the working fluid and the valve, since all of them have motion in vertical direction. The viscosity however, does not change at all. This also implies that Froude scaling is more relevant than Reynolds and therefore, will be used in the remaining of this research.

4.4 Distorted Models

In both the Froud and the Reynolds models, lengths are scaled with the scale ratio (L_r) and areas scale quadratically (L_r^2). In practice, this means that if the length of one of the pipes in the SPP is increased with a factor thirty, the diameter increases with the same factor, and the area increases with a factor nine hundred. Distorted models work differently and assume that the length and the diameter do not necessarily have the same scaling. So in the case of a distorted model, the diameters of a pipe does not necessary change with the same ratio as the length of the pipe. However, both Froude models as Reynolds models, do not provide

adequate theory to calculate the difference in ratio. Therefore, it will be a case of trial and error with different scaling on the diameter and length, to come up with the optimal ratio.

5. The Single-Piston Pump Model

As described earlier, an experimental setup of the SPP has been developed and is located at the Ocean Grazer water hall. This prototype is the first experimental setup of the pumping system and has been made by van Rooij [8]. Over the years the experimental setup has been improved and in January 2018 the thesis of Zaharia resulted in a new designed mathematical simulation model [9]. This new design is used the determine and describe the behaviour of the SPP and is a combination of MATLAB-scripts, and Simulink. Simulink uses physical components which can be connected to each other. The physical blocks used are:

- The reservoir
- The valves
- The piston
- The motor
- The piping
- The pulley

Running the model results in the following output:

Table 4: Results Simulink Model

Average Max displacement	1 meter
Total Pumping energy	3118.88 Joule
Total Potential energy	958.76 Joule
Avg. Pumping energy per stroke	1039.62 Joule
Avg. Potential energy per stroke	319.58 Joule
Volumetric Efficiency	82.93 %
Mechanical Efficiency	37.07 %
Total Efficiency	30.74 %

Furthermore, multiple forces, pressures, energies, flows and positions are calculated and plotted demonstrating the behaviour of the SPP.

The design proposed in the thesis of Zaharia has the limitation that it cannot be used to scale up the SPP directly. Therefore, more research has to be done on the influence of the effect of scaling. Within the SPP model, a MATLAB-script is used to clarify the parameters and assign a value to them. The problem that occurs, is that the parameters described in the MATLAB-script cannot be scaled up straightforwardly. Consequently, appropriate scaling laws are necessary to give the parameters a correct scaling.

6. The MATLAB-Script

The MATLAB-script of the model is divided is multiple sections, that represent the different parts of the SPP. The different sections are described and explained below.

6.1 Switches and Changeable Parameters

In this section the number of balls in the check valve and piston valve are defined. The balls open the holes in the check valve when the piston is moving upwards and closes them when it moves downwards. The same action, only vice versa, happens in the piston valve. The number of balls depend on the total passage area of the valves and the size of the balls. With a larger passage area, there should be more balls or bigger balls in order to keep the flow ratio constant. The initial number of balls is stated in appendix A and B. Most important is that the total valve areas as the total passage areas are proportional to each other and scale according to L_r^2.

6.2 Simulation Parameters

The simulation parameters stated in the MATLAB-script consist of "the density of the working fluid" and the "gravitational constant". Both parameters are constants since the density of the working fluid will not change when the volume of the SPP is scaled up, the same holds for the gravitational constant.

6.3 Motor Parameters

The three parameters of the motor that need to be scaled are the amplitude, the frequency and the time range. The amplitude is the distance from the equilibrium position of the motor to its maximum deviation. This amplitude is a length and will be multiplied with L_r. The frequency is defined as $\frac{rad}{sec}$ and since times scales with $\sqrt{L_r}$, the frequency will scale with $\frac{1}{\sqrt{L_r}}$. Furthermore, the time range need to be extended to fit in the same amount of strokes. The time range will be multiplied with $\sqrt{L_r}$.

6.4 Reservoir Data

The parameters of the reservoir stated in appendix D are based on length, width, height, area and volume. Length, width and height have meter as their dimension and scale linearly (L_r), area has square meter as dimension and scales with L_r^2, volume is defined in cubic meter and scales according to L_r^3. In the case of the reservoir parameters, the areas and volumes are calculated by means of length, width and height. Consequently the areas and volumes are scaled automatically and do not need to be scaled separately.

6.5 Piping Data

As stated in appendix D, the data of the piping system depends on length, width, height, area, radius, angle and flow discharge. Length, width, height and radius are measured in meter and therefore, scale linearly (L_r). The area scales quadratically (L_r^2) , however in the piping data the area is calculated with linear parameters, and therefore, it needs no direct scaling. The dimension of the flow discharge is $\frac{m^3}{s}$ and is stated as a value, instead of a

calculation based on linear parameters. The equality of the Froude number is used to calculate the flow discharge ratio,

$$Q_r = L_r^{5/2}, \tag{32}$$

where Q_r in the flow discharge ratio and L_r the length ratio. Consequently, it is possible to calculate the flow discharge of the scaled SPP,

$$Q_p = Q_m \, Q_r \tag{33}$$

where Q_m is the flow discharge of the experimental setup and Q_p is the flow discharge of the prototype. Furthermore, scaling has no influence on the angel of bend.

6.6 Check Valve Data

In the check valve data, the characteristics of a single ball are described. If the same balls are used, only in bigger numbers, that values will stay the same. If the balls are scaled with Froude, the passage area radius will scale linearly (L_r) and the areas will scale quadratically (L_r^2). Furthermore there has to be dealt with a ''cracking pressure'' and a ''maximum opening pressure''. The following laws are applied,

$$p_r = L_r \tag{34}$$

where p_r is the pressure ratio and

$$p_p = p_m \, p_r. \tag{35}$$

Consequently, the pressure values should be multiplied with the length ratio and therefore, scale linearly.

6.7 Piston Pump Parameters

The parameters of the pump consist of lengths, masses, areas, Young's modulus, a rod damping ratio, stiffness factors and damping factors. The length defined in the piston pump parameters, is a sum of the single pipe lengths. Since all the single pipes are scaled in the piping data, the total pipe length does not require any scaling.

The masses are split up in the mass of the piston/rod and the mass op the pipes. The mass of the pipes is based on the radius of the pipes, the length of the pipes and the density of the working fluid. The density of the working fluid is a constant and will not change. The lengths and radii of the pipes, are the ones defined in the piping parameters. They will scale linearly (L_r) and consequently, the mass will scale according to their scaling. The mass of the piston/rod is defined as a number and therefore, this mass will scale to the power of three (L_r^3).

The length and radius of the rod are difficult to scale. The length of the rod depends on the distance between the floater and the piston. This distance is based on the depth of the

ocean and the water level and therefore, it has no relation with the other parameters. The radius of the rod is related to the forces it has to cope with. Therefore, the larger the force that acts on the cable, the thicker the cable has to be.

Another constant that has to be determined is the stiffness factor of the rod (k_{rod}). The stiffness factor depends on the radius of the rod, the Young's modulus of steel and the length of the rod, and is defined as:

$$k_{rod} = \frac{\pi R_r^2 E_{st}}{L_r}. \tag{36}$$

The radius of the rod and the length of the rod both scale linear and the Young's modulus has the dimension $[N/m^2]$. Since π is dimensionless, the stiffness factor defined in its dimensions equals,

$$k_{rod} = \frac{m^2 \frac{N}{m^2}}{m} = \frac{N}{m} = \frac{Lr^3}{L_r} = L_r^2 \tag{37}$$

which implies that the K factor scales quadratically. Nevertheless, it is unlikely that the radius and the length of the rod scale with the same ratio. Therefore the K factor of the rod cannot be scaled straightforwardly.

The damping coefficient of the rod is defined as:

$$c_{rod} = 2\zeta \sqrt{\mathrm{m_p\ k_{rod}}} \tag{38}$$

where ζ is the rod damping ratio, m_p is the mass of the piston and K is the stiffness factor. Assuming the K factor scales quadratically ,the mass scale to the power of three and the rod damping ratio is dimensionless, c_{rod} defined in its dimensions equals,

$$c_{rod} = \sqrt{L_r^3\ L_r^2} = L_r^{\frac{5}{2}}. \tag{39}$$

Furthermore, the water columns itself also behaves as a spring-damper system. The damping of the water column is defined as,

$$c_{water} = 2m_f\ \omega_f\ \zeta_f \tag{40}$$

where m_f is the mass of the working fluid and is calculated as,

$$m_f = \sum \rho\ A\ l. \tag{41}$$

The natural frequency ω_f, with l as the length of the piping, is defined as,

$$\omega_f = \sqrt{\frac{2\ g}{l}} \tag{42}$$

and ζ_f is the damping ratio of the water column.

The spring in the water column is determined by,

$$k_{water} = 2\,\rho\,A\,g \tag{43}$$

where ρ is the density of the working fluid, A is the surface area of the piping and g is the gravitational constant.

An important side note is that the spring and damper coefficients described above are not used at all in the Simulink model. Values for the spring and damper are found by trial and error and are not based on calculations.

6.8 Valve in Piston Parameters

The piston valve is very similar to the check valve. When the SPP is scaled up and the same balls are used, the pressures, the radius and the areas will not change. If bigger balls are used to cover the passage area, research has to be done on the characteristics of these new balls. However according to Froude, the diameters of the balls scale linearly (L_r), whereas the areas scales quadratically (L_r^2). Furthermore, their pressures will scale linearly (L_r) as well.

7. Relevant Parameters and Outputs

7.1 Diameter and Length

The diameter and length of the pipes can be scaled in two ways. The first way is to scale the diameter and the length with the same factor, which is concerning geometric similarity, the most common way. Second, the diameter can be scaled with a different ratio than the length, which is called a distorted model. When a distorted model occurs, it is more likely that the diameter has a smaller scaling ratio than the length. There is no specific theory on the scaling of distorted models, but it will be of influence on the output of the model. When the length is scaled with a ratio larger than the ratio of the diameter, the ratio between volume and area of the valves also becomes larger. Consequently, to ensure a consistent flow through the valves, the velocity through the valves has to increase.

7.2 The Passage Area

The total passage area is proportional to the diameter of the valves. To ensure that the discharge and velocity of the working fluid through the valves, scale along Froude, the passage area should increase quadratically with the ratio of the length (L_r^2). However, if the diameter of the piston pipe scales with a smaller ratio than the length of the pipe, the Froude laws for discharge do not apply. The volume of the piston pipe is defined by,

$$V = \pi\, Y^2\, X \tag{44}$$

where Y is the radius of the pipe and X the length of the pipe. Consequently, if Y and X scale with the same ratio, the volume increases with this ratio to the power of three (L_r^3). Furthermore if the length scales with a higher ratio than the diameter, the volumes increases with the scaling ratio of the diameter to the power of two (D_r^2) multiplied with the ratio between the new and the old length of the pipe. Hence, the ratio between the volume of the piston pipe and cross-sectional area of the piston pipe, increases when the length of the pipe is scaled with a higher ratio than its diameter. This means, that if the time set for one upstroke and one downstroke scales with Froude, the discharge through the valves increase with the diameter ratio to the power of two and half $(D_r^{\frac{5}{2}})$, multiplied with the ratio between the new length and the old length of the pipe.
So normally the discharge is defined as,

$$Q = V\, A \tag{45}$$

where Q is the discharge in (m^3/s), V is the velocity in (m/s) and A is the passage area in m^2. Therefore, the scaling of the discharge according to Froude is stated as,

$$Q\, L_r^{\frac{5}{2}} = \left(V\, \sqrt{L_r}\right)\, (A\ \ L_r^2). \tag{46}$$

Except in the case of a diameter that scales with a ratio smaller than the length ratio, it is defined as,

$$Q\ D_r^{\frac{5}{2}}\ \frac{L_r}{D_r} = (V\sqrt{D_r}\ \frac{L_r}{D_r})\ (A\ \ D_r^2). \tag{47}$$

The value of $\frac{L_r}{D_r}$ is always bigger than 1 if the diameter scales with a smaller ratio than the length. Therefore, compared to normal Froude scaling where $D_r = L_r$, there is an increase in discharge and velocity of the working fluid.

Furthermore, the efficiency decreases when the SPP is scaled up, even though the scaling equations are implemented. However, an efficiency that is comparable to that of the SPP can be ensured, but only if the passage area is increased with a ratio higher than L_r^2 or D_r^2, depending on the scaling of the diameter and length of the piping. Eventually, this will be problematic, because to passage area will become too big to fit in the total valve area.

7.3 Size and Number of Balls

The passage area is opened and closed by balls. When the total passage area increases, there are two option to regulated the flow. The first option is to increase the number of balls, in this case the cracking pressure will be equal to the pressure used in the MATLAB-script. A second option is to enlarge the holes in the valves and use bigger balls to cover the passage area. The use of bigger balls is more difficult, because the cracking pressures and maximum opening pressures will be different than the ones used in the MATLAB-script. However, presumably it is necessary to use bigger balls, because the balls used in the MATLAB-script, seem to bounce if a much higher volume per second is pushed through the passage areas. The bouncing of the balls causes a much higher piston force in the down-strokes and disturbs the flow through the check valve. Therefore the diameter of the balls are scaled linearly (L_r).

7.4 Cracking Pressure and Maximum Opening Pressure

The cracking and maximum opening pressure need to be determined with trial and error and are very important to determine correctly. If the pressures are too high, the holes will not open at all or not completely and the desired flow will not be achieved. On the other side, if the pressures are too low, the balls go up rapidly and will bounce back. This will happen over and over again, resulting in constant bouncing of the balls. The bouncing causes problems in the flow over the check valve. In this research the equations (34) and (35) are applied and the pressures will scale linearly (L_r).

7.5 Spring and Damper

In the case of spring and damper two situations reveal themselves. The first situation is the one used in the Simulink model, where the two values for the spring and the damper are determined by trial and error. With different scaling, these values could be determined again with trial and error, until the values that give the most appropriate output are defined. A different approach is to have a closer look at its dimension. Both spring and damper are defined by $\frac{N}{m}$, whereas according to Froude, force (N) scales to the power of three (L_r^3) and meter (m) scales to the power of one (L_r). Resulting in the assumption that both the spring as the damper scale quadratically with the ratio of the length (L_r^2).

In the second situation, the formulas, to determine the spring and damper values, are used. The spring factor for the rod is calculated with,

$$k_{rod} = \frac{\pi R_{rod}^2 E_{st}}{L_{rod}}. \quad (48)$$

Since the Young's modulus is constant, k_{rod} depends completely on the ratio between radius and length. The length of the rod is determined by the distance between piston and the floater and is therefore, dependant on the water level of the ocean. Hence, the length of the rod has less to do with the scaling of the model and therefore, k_{rod} is cannot be scaled straightforwardly.

The spring of the water column (k_{water}) is defined by,

$$k_{water} = k_{up} + k_{down} = \rho\, g\, A_{up} + \rho\, g\, A_{down}. \quad (49)$$

Therefore, k_{water} can be scaled up quadratically if the scaling ratio of the diameter of the pipes is determined.

The damping of the rod is defined by,

$$c_{rod} = 2\zeta \sqrt{\mathrm{m_p\ k_{rod}}}, \quad (50)$$

where the mass of the piston (m_p) can be increased with the length ratio to the power of three (L_r^3) or with the diameter ratio to the power of two (D_r^2) multiplied with the length ratio to the power of one(L_r), if the diameter and length are scaled with a different ratio. However, as explained earlier, k_{rod} depends on the water level of the ocean and thickness of the rod, which are not scalable. Therefore the damping of the rod is not scalable as well.

The damping of the water column is determined by,

$$c_{water} = 2m_f\, \omega_f\, \zeta_f \quad (51)$$

The mass of the working fluid (m_f) is proportional to both the length as the diameter of the piping, whereas the natural frequency (ω_f) only depends on the length. Consequently, the damping of the water column needs to be recalculated if the SPP is scaled. The Froude law can be used for the scaling of the mass and natural frequency if both the length and the diameter scale with the same ratio. If the diameter and length scale with a different ratio, the mass needs to be scaled with the scaling ratio of the diameter to the power of two (D_r^2) multiplied with the ratio between the new and the old length of the pipe.

7.6 The Slamming Frequency

In the experimental data, oscillations occur when force is plotted with respect to time. The reason behind the oscillations is the phenomenon called slamming. When the piston moves up and down, it causes movement of the working fluid. The working fluid flows through the pipes and slams against the pipe walls, causing vibrations. Furthermore, the balls in the

valves open and close until they are fully opened, which also causes vibrations. The vibrations reveal themselves as oscillations in the force output.

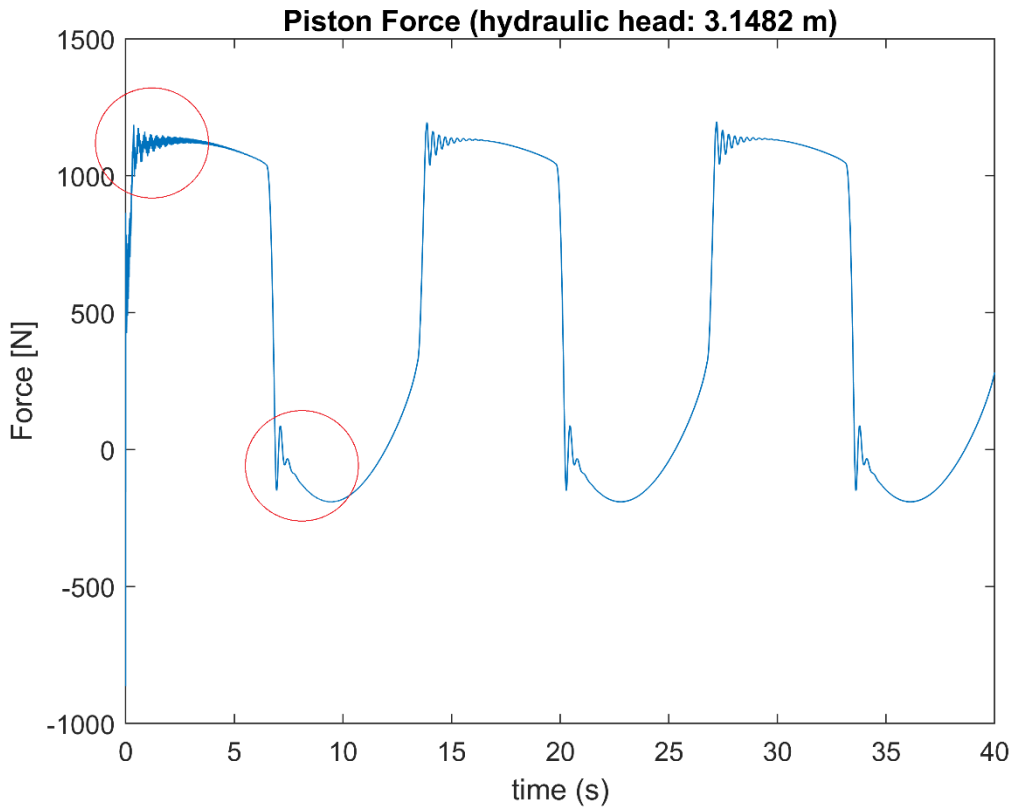

Figure 8: Force/time, including oscillations in the up and down strokes

In figure 8, the oscillations in the first up and downstroke are indicated with a red circle. The force goes below the zero point due to the piston that goes downwards with a lower velocity than the rod. The frequency of the slamming is calculated with,

$$\omega = \sqrt{\frac{k}{m}} \tag{52}$$

where k is a spring factor defined as,

$$k = k_{rod} + k_{water}. \tag{53}$$

The different k factors are defined as,

$$k_{rod} = \frac{\pi R_r^2 E_{st}}{L_{rod}} \tag{54}$$

and

$$k_{water} = k_{up} + k_{down} \tag{55}$$

where R_r is the radius of the rod and L_{rod} is the length of the rod.

The factors k_{up} and k_{down} are defined as,

$$k_{up} = \rho\, g\, A_{up}, \tag{56}$$

and

$$k_{down} = \rho\, g\, A_{down}. \tag{57}$$

Furthermore, m is the mass of the working fluid column and is characterized as,

$$m = \rho\, \pi\, r^2\, h \tag{58}$$

It becomes clear that the k factor depends on the area of the pipe, whereas the mass is depends on both the area as the length of the pipe. Therefore if the diameter and length scale with the same ratio, the scaling of the frequency is defined as,

$$\omega_r = \sqrt{\frac{L_r^2}{L_r^3}} = \frac{1}{\sqrt{L_r}} \tag{59}$$

If the length scales with a different ratio than the diameter, the scaling of the frequency is defined as,

$$\omega_r = \sqrt{\frac{D_r^2}{D_r^2\, L_r}} \tag{60}$$

Consequently, the frequency decreases in both cases, only the frequency decreases even more if the length scaling ration is larger than the diameter scaling ratio, because the volume increases in proportion to the area.

8. Results and Discussion

In the following chapter, normalized piston force, the displacement of the piston/amplitude of the motor, the potential energy, the pumping energy and the efficiencies are compared with different scaling. In the first case of every paragraph, the diameter and length scale with the same ratio, [1:X], whereas in the second case, the diameter ratio will always be one third of the length ratio, [1:X:X/3]. Furthermore, the number of balls in the valves stay equal. Therefore, in first cases the passage area, cracking pressure and maximum opening pressure will scale with the length ratio, where in second cases, they will scale along the diameter ratio.

8.1 The Normalized Piston Force

The piston force is divided by $(\rho\ g\ \Delta H\ A)$, in this case the differences due to mass of the hydraulic head are taken out, and the value on the Y-axis becomes a dimensionless number. This value is plotted over time divided by its period. Therefore, the X-axis is also dimensionless and the influence of scaling can be compared more easily.

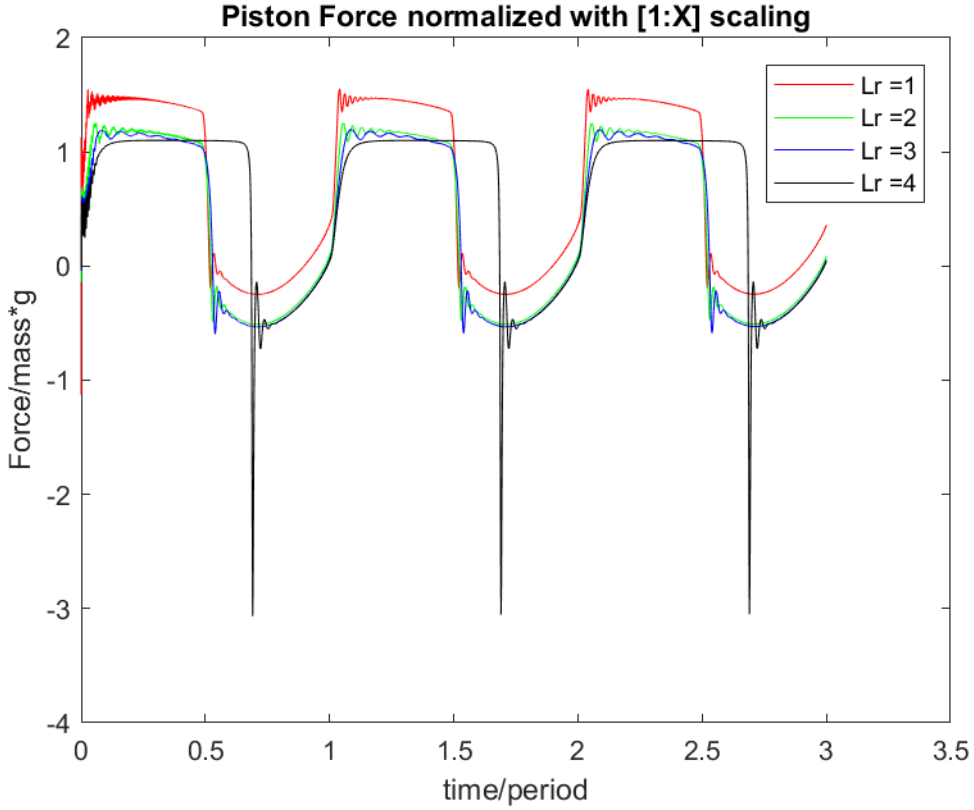

Figure 9: Normalized piston force against time/period and [1:X] scaling

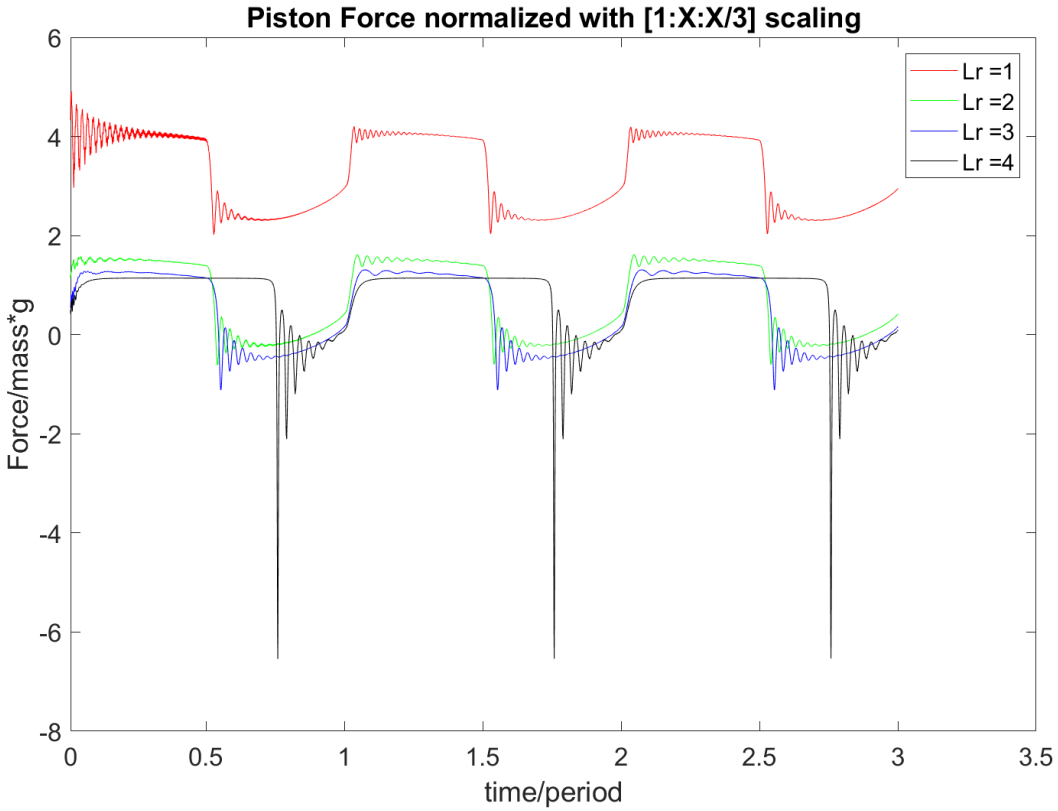

Figure 10: Normalized piston force against time/period and [1:X:X/3] scaling

The piston force is defined as,

$$F_p = A_t[\rho\, g(L_c + L_u - L_l) + \rho(L_c + L_u)\ddot{z}_p + \rho \dot{z_p}^2] \tag{61}$$

where A_t is the time variation of the open area of the check valve, L_c is the length of the cylinder between both reservoirs, L_u and L_l are the water depth of the upper and lower reservoirs and ρ is the density of the working fluid. The first term inside the brackets in equation (57) represents the pressure due to the hydraulic head between two reservoirs, the second term accounts for the inertia of the working fluid in the cylinder, and the third term describes the dynamic pressure of the working fluid [14]. Because the force is divided by the mass of the hydraulic head multiplied with the gravitational constant, the influence of the pressure due to hydraulic head between the two reservoirs is taken out. This results in, except for (L_r=1), that the peaks of the upstrokes are roughly around one. Which indicates that the influence of the inertia of the working fluid and the dynamic pressure of the working fluid are almost neglectable, except for the case (L_r=1). Therefore, the force is scales with the same ratio as the mass (L_r^3), which is according to the Froude scaling. The forces go below the zero point due to the fact that the piston is not capable to go downwards with the same velocity as the rod. With higher scaling ratios, the distance that the piston and rod have to travel downwards increases and the difference in velocity becomes more of an influence. Therefore, the negative force becomes larger with higher scaling ratios. The large oscillations in the downstroke of (L_r=4) are due to high positive pressure differences in the piston valve and high negative pressure differences in the check valve. Furthermore, the slamming frequency in the upstroke decreases, according to equation (56) and (57).

8.2 Displacement of the Piston in Proportion to the Motor Amplitude

The displacement of the piston is divided by the amplitude of the motor, hence, it becomes a dimensionless number. It will show the difference between the piston displacement and the amplitude of the motor. Furthermore, on the X-axis, the time is divided by the period, so it becomes a dimensionless number as well.

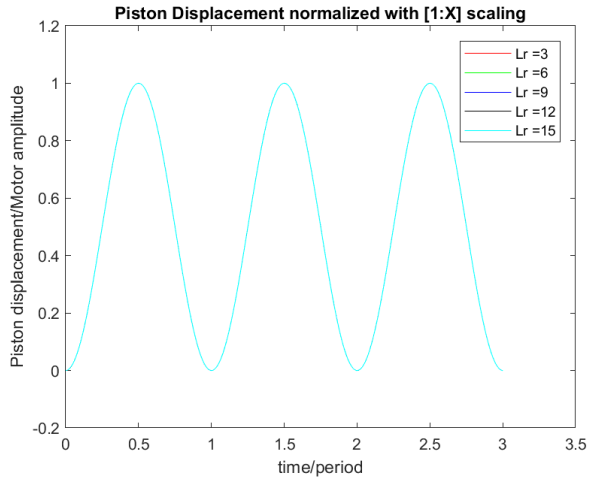

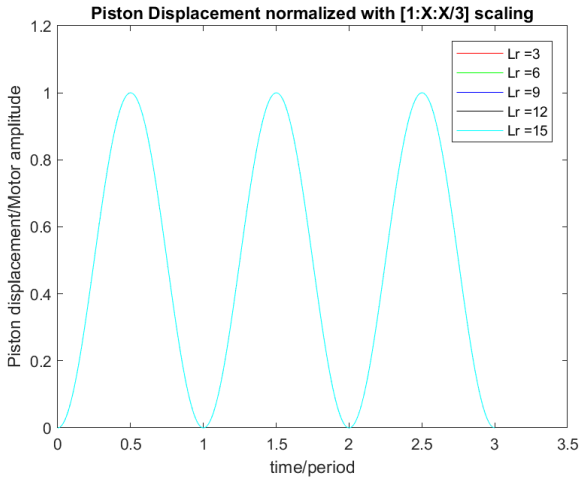

Figure 11 and 12: Piston displacement normalized against time/period with [1:X] and [1:X:X/3] scaling

Comparing figure 11 and figure 12, it is clear that the ratio between the piston displacement and the amplitude of the motor is around one with different scaling, which is logically, because the piston follows the motion of the motor. Consequently, if the motor amplitude is scaled, the piston displacement should scale with the same ratio. The plots of $(L_r = 3,6,9,12)$ are not visible because they are overlapped by the plot of the length scaling ratio of fifteen. Furthermore, it results in the conclusion that scaling the diameter with a different ratio than the length does not have any influence on the ratio between piston displacement and motor amplitude,

8.3 Potential energy over different scaling

In the tables below, the measured potential energy over a length scaling ratio from one till four, is subtracted from the mathematical simulation model. The only difference is that in table 4 the diameter and length scale with the same ratio, and in table 5 the diameter is one third of the length. The amount of potential energy is proportional to the volume of the working fluid that has been pumped from to lower reservoir to the higher reservoir. The difference in potential energy is consistent with the fact that the potential energy depends on the volume of working fluid pumped from the lower to the higher reservoir. In the case of [1:X] scaling, the diameter of the piping is three times as large as in than in the case of the [1:X:X/3] scaling and thus, the volume is bigger. The reason why larger scaling is not used will be discussed in the discussed in chapter 9.

Furthermore, according to theory, energy can be scaled with the length scaling ratio to the power of four (L_r^4). In table 4 and 5, the simulated potential energy of the SPP model is compared with the calculated potential energy. The potential energy of the [1:1] situation is

multiplied with (L_r^4), which result in that the simulated and calculated potential energy, with length scaling ratio of two and three, are roughly the same. However, the simulated and calculated potential energy of (L_r=4) is completely off, probably due to errors in the model which will be discussed in chapter 9. In conclusion, for a rough estimation, the potential energy is scalable with Froude. Yet, there is always a substantial difference which becomes critical in calculating the total efficiency.

Table 5: Total potential energy simulated and calculated with [1:X]

Scaling [$\boldsymbol{L_r}$]	Total potential energy [J] [1:X]	Calculated total potential energy [J] [$\mathbf{1}:\mathbf{1}].\boldsymbol{L_r^4}$	Difference [%]
1	959	959	
2	14,918	15,340	2.83
3	71,681	77,660	8.34
4	107,795	245,443	127.69

Table 6: Total potential energy simulated and calculated with [1:X:X/3]

Scaling [$\boldsymbol{L_r}$]	Total potential energy [J] [1:X:X/3]	Calculated total potential energy [J] [$\mathbf{1}:\mathbf{1}:\mathbf{1/3}].\boldsymbol{L_r^4}$	Difference [%]
1	119	119	
2	1,973	1,904	-3.50
3	9,896	9,639	-2.60
4	14,764	30,464	106.34

8.4 The Pumping Energy

In table 6 and 7 the simulated pumping energy of the SPP models of the is compared with the calculated pumping energy. The same principle as in 8.3 is used to calculate the pumping energy. Notable is that the calculated pumping energy is roughly the same as the simulated pumping energy and therefore, the pumping energy seems to be scalable with Froude. However, there is always a small difference between the simulated and calculated energies, which is critical in calculating the total efficiency. Furthermore, the measured and calculated pumping energy of (L_r=4) are again, not coherent, which will be discussed in chapter 9.

Table 7: Pumping energy simulated and calculated with [1:X]

Scaling [$\boldsymbol{L_r}$]	Pumping energy [J] [1:X]	Calculated pumping energy [J] [$\mathbf{1}:\mathbf{1}].\boldsymbol{L_r^4}$	Difference [%]
1	3,119	3,119	
2	49,230	49,904	1.37
3	238,591	252,639	5.89
4	412,528	798,464	93.55

Table 8:Pumping energy simulated and calculated with [1:X:X/3]

Scaling [L_r]	Pumping energy [J] [1:X:X/3]	Calculated pumping energy [J] [$\mathbf{1}:\mathbf{1}:\mathbf{1}/\mathbf{3}].L_r^4$	Difference [%]
1	336	336	
2	6,380	5376	-15.74
3	32,105	27,216	-15.23
4	48,950	86,016	75.72

8.5 Efficiencies

In the tables below, the volumetric, mechanical, and total efficiencies are compared. In table 7 the diameter and length scale with the same ratio, whereas in the table 8, the diameter ratio will always be one third of the length ratio.

Table 9: Efficiencies with [1:X] scaling

Scaling [L_r]	$\eta_{volumetric}$ [%]	$\Delta_{volumetric}$ [%]	$\eta_{mechanical}$ [%]	$\Delta_{mechanical}$ [%]	η_{total} [%]	Δ_{total} [%]
1	82.93		37.07		30.74	
2	80.56	-2.85	37.61	1.47	30.30	-1.42
3	76.44	-5.12	39.30	4.49	30.04	-0.86
4	36.34	-52.45	71.90	82.93	26.13	-13.03

The volumetric efficiency decreases with larger scaling, whereas the mechanical efficiency increases. The total efficiency is a multiplication of the volumetric and mechanical efficiency, and since the increase in mechanical efficiency is less than the decrease in volumetric efficiency, the total efficiency decreases. Noticeable is the big difference between the length scaling ratio of three and four. This is probably the result of errors in the model, consistent with the potential energy, which is not scalable with a length ratio of 4.

Table 10: Efficiencies with [1:X:X/3] scaling

Scaling [L_r]	$\eta_{volumetric}$ [%]	$\Delta_{volumetric}$ [%]	$\eta_{mechanical}$ [%]	$\Delta_{mechanical}$ [%]	η_{total} [%]	Δ_{total} [%]
1	93.99		37.78		35.51	
2	96.20	2.34	32.15	-14.89	30.93	-12.89
3	95.23	-1.00	32.37	0.66	30.82	-0.34
4	44.91	-52.84	67.15	107.48	30.16	-2.15

The continuity of a decreasing volumetric efficiency and an increasing mechanical efficiency does not hold when the diameter and length are scaled with a different ratio. However, the decrease in total efficiency is consistent. This consistent decrease claims that the total potential energy and pumping energy in 8.3 and 8.4 are not scalable with Froude, since the total efficiency is defined as,

$$\eta_{total} = \frac{total\ potential}{pumping\ energy}\ 100 \tag{62}$$

If both the potential energy as pumping energy are scaled according theory, the total efficiency would stay the same as in the [1:1] situation.

8.6 Limitations

During this research multiple limitations of the SPP model revealed themselves. The first limitation is that for scaling with a high number the model does not hold and results in outputs that are not useful. The meaningless output is due to the potential energy that is not scalable with a length scaling ratio larger than three, and which goes below zero after the length ratio involves a number of five or higher. The potential energy is directly related to the total efficiency and the mechanical efficiency, hence their value becomes irrelevant as well.

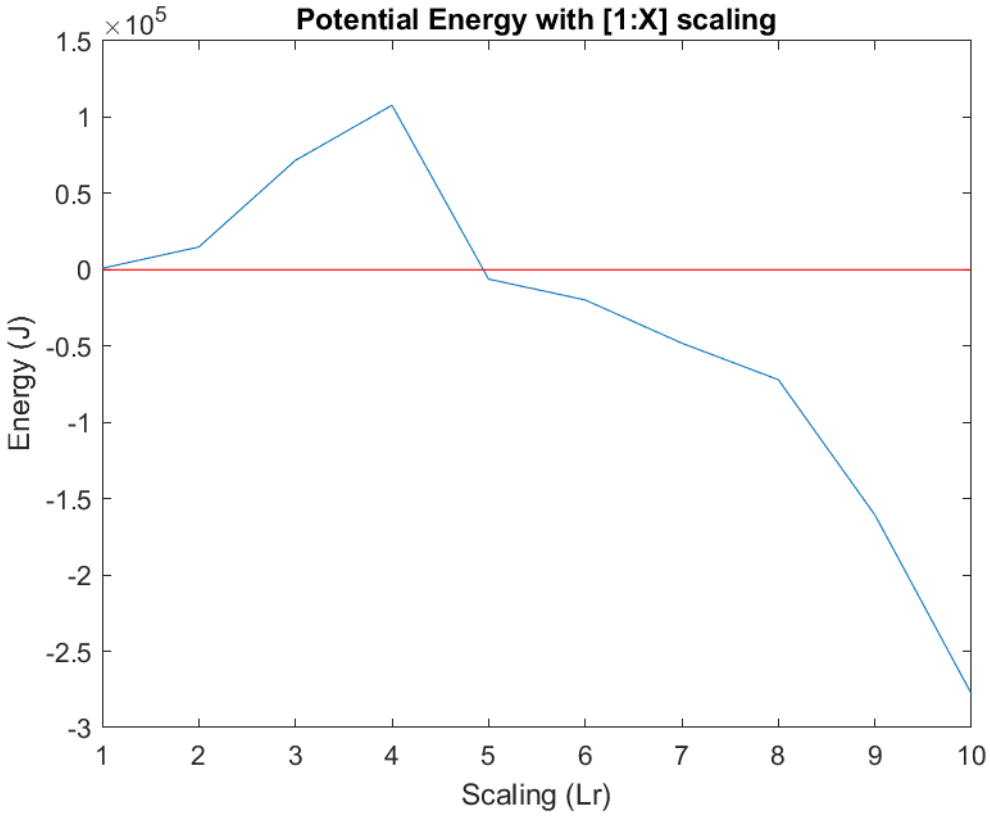

Figure 13: Potential energy against different scaling with [1:X] scaling

The reason behind the negative potential energy is the flow through the check valve. Normally the flow through the check valve is maximum in the upstroke, when the passage area of the check valve is maximum opened, and minimum in the downstroke, when the passage area is closed. In figure 14 the flow though the check valve is compared with a length scaling ratio of three, four and five. With a length scaling ratio of four, the check valve already has some leakage in the downstroke, which explains the errors with a length scaling of four in chapter 8. However, the overall shape of the of the length scaling ratio of four is still correct, with an increasing flow in the upstroke until it is maximum. The shape of the flow through the check valve with a length scaling ratio of five is completely off, with heavy oscillations

during the up and downstroke. Increasing the cracking pressure, the maximum opening pressure and the passage area does influence the flow and the oscillations, yet the heavy oscillations do not disappear. The heavy oscillations are probably due to the bouncing of the balls, however it is inexplicable why to bouncing cannot be stopped with the increases of the pressures and size of the balls or why it suddenly occurs after an length ratio of five or more.

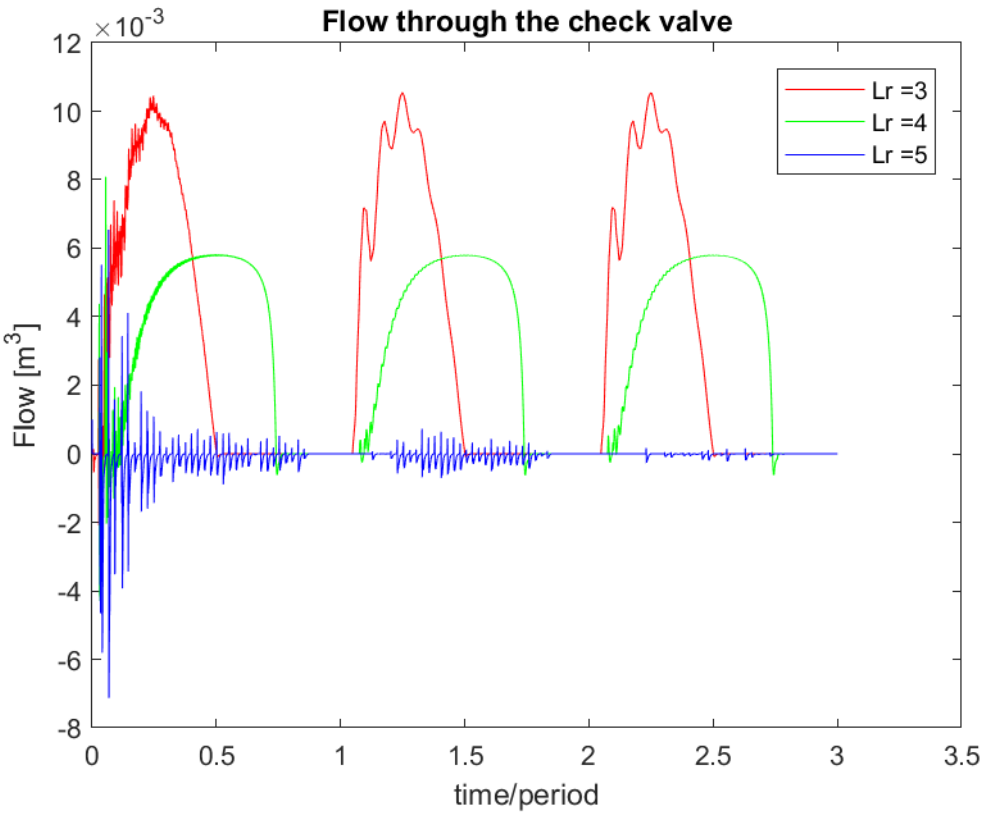

Figure 14: Flow through the check valve with [1:X] scaling

There is no clear reason for the issues in the model, however, Zaharia acknowledged that it is most likely that there are multiple small errors in the initial parameters. The difficulty about these errors is that Zaharia is sure about their existence, but even he, the developer of the model, does not know where the errors occur. The most plausible reason behind the limitations of the model, is that when the model is scaled with a small scaling ratio, the errors will not be of a big influence. However, when the model is scaled with a higher scaling ratio, the errors will increase as well. At some point the errors will be of such influence that the output of the model is disrupted, which is clearly from a length scaling ratio of 4 or higher.

Furthermore, the check valve was adjusted in multiple ways in order to solve the oscillation problem. However, using less, but bigger balls or changing the pressures of the balls, does not solve the problem. Additionally, the whole check valve was removed, which resulted in more irrelevant output. When the check valve is removed, the piston, when in downstroke, pushes the working fluid back to the lower reservoir. Nevertheless, to solve the scaling problems of the mathematical simulation model, it is critical to fix the problems with the flow through the check valve. One of the basic assumptions and limitations of check valves

in Simulink, is that it does not take into account any loading on the valves, such as inertia, spring and friction. However, the spring coefficient of the rod is increasing quadratically and the spring coefficient of the water columns will also increase quadratically, but is not taken into consideration in the SPP model. Both of them will be of influence and therefore, the check valves of Simulink are probably not suitable anymore if the system is using high spring coefficients.

9. Conclusion and Recommendations

Throughout this research, the mathematical simulation model is adjusted according to appropriate scaling laws. Thereafter, the model is used to predict multiple outputs, such as the efficiencies, energies, displacements and forces. These values analysed and compared with the outputs according to the scaling theory, which lead to several conclusion about the scaling effects and scalability of the mathematical simulation model.

First of all, the normalized piston force is compared using different scaling ratios. It becomes clear that the piston force mainly depends on the pressure between the two reservoirs due to hydraulic head. Therefore, the piston force is scalable with the Froude theory. The Froude multiplication factor is based on the mass and therefore the force needs to be multiplied with L_r^3. However, the normalized force with $(L_r = 1)$ behaves differently, concluding that in the [1:1] situation, the inertia and the dynamic pressure, of the working fluid, are more of an influence. Furthermore, the slamming frequency scales with Froude law.

Secondly, the displacement of the piston is compared to the amplitude of the motor, which results in similar plots for both [1:X] and [1:X:X/3] scaling. Moreover, the peaks of both plots are around one, which indicates that the piston displacement and the amplitude of the motor are directly related to each other. Consequently, linear scaling of the motor amplitude result in linear increase of the piston displacement.

Thirdly, the measured total potential energy and pumping energy were subtracted from the mathematical simulation model and compared with the energies calculated with the Froude law. For length scaling ratios that are considered low, the total potential energy and the pumping energy can approximately be determined with increasing the energy of the [1:1] situation with the Froude multiplication factor of energy. The calculated energies are broadly the same as the measured energies, but never completely accurate. This becomes problematic in calculation of the total efficiency, because in the case of calculated energies, the total efficiency is similar for different scaling, whereas the mathematical simulation model clearly shows that the efficiency should decrease. This proves that the scaling effects influence the energies, such that they cannot be scaled according to the Froude law.

Overall, the mathematical simulation model can be used to predict the efficiency for low scaling ratios. However, length scaling ratios that exceed the value of three result in irrelevant outputs, due to the oscillations in the flow over the check valve. Therefore, in the current condition, the mathematical simulation model is not capable to predict the total efficiency of the full-scale single-piston pump. The calculated potential and pumping energy can also not be used to derive the total efficiency, because the calculated energies assume that the total efficiency stays constant, which is wrong.

It is recommended that first, the initial parameters are compared with the dimensions of the experimental setup, in order to eliminate every tiny error in the initial parameters. If the initial parameters are completely free of errors, the outputs will become more relevant. Second, it should be wise to do more research on the check valve. The check valve is the bottleneck

in the mathematical simulation model and need to be adjusted or replaced to ensure more adequate results. Furthermore, the normalized piston force in the case of $(L_r = 1)$ is considerably higher than the ones of $(L_r = 2,3,4)$. Therefore, research on the scaling effects of the inertia and dynamic pressure, of the working fluid, is recommended and would result in even more precise predictions of the force.

Reference List

[1] Cossia, Juliann M. 2011. *Global warming in the 21st century*. New York: Nova Science Publishers, Inc.

[2] World energy council. 2016. *World energy resources|2016*. URL: https://www.worldenergy.org/wp-content/uploads/2016/10/World-Energy-Resources-Full-report-2016.10.03.pdf

[3] Communication from the Commission to the European Parliament, the Council, The European Economics and Social Committee and the Committee of the Region. *A policy framework for climate and energy in the from 2020 up to 2030.* URL: https://ec.europa.eu/energy/en/topics/energy-strategy-and-energy-union/2030-energy-strategy

[4] U.S. energy information administration. 2017. *Renewable energy explained.* URL: https://www.eia.gov/energyexplained/?page=renewable_home'

[5] Vakis, Antonis I., and John S. Anagnostopoulos. 2016. *Mechanical design and modeling of a single-piston pump for the novel power take-off system of a wave energy converter.* Renewable Energy 96 (Part A): 531-547.

[6] The Ocean Grazer company. 2018. *Ocean grazer website*. URL: http://www.ocean-grazer.com/

[7] Towery, Nate D, Elizabeth Machek, Anthony Thomas, Zachary Ellis, David Kuehn, John A. Volpe National Transportation Systems Center (U.S.), and United States. Federal Highway Administration. 2017. *Technology Readiness Level Guidebook.* McLean, VA: United States Department of Transportation, Federal Highway Administration.

[8] van Rooij, M. 2015. *Experimental validation of dynamical contact models of the ocean grazer.* [Master of Science]. Rijksuniversiteit Groningen.

[9] Zaharia, RM. 2018. *Understanding of the single-piston pump inside the ocean grazer.* [Master of Science]. Groningen: Rijksuniversiteit Groningen.

[10] Prins, W.A. 2016. *Business system design.* [Bachelor Course]. Groningen: Rijksuniversiteit Groningen.

[11] van Strien, Pieter J. 1997. *Towards a methodology of psychological practice : The regulative cycle*. Theory & Psychology 7 (5): 683-700.

[12] Jackson, Michael C. 2003. *Systems thinking : Creative holism for managers*. Chichester, West Sussex ;: John Wiley & Sons,.

[13] Chanson, Hubert. 2004. *Hydraulics of open channel flow*. Vol. 2nd ed. Amsterdam: Butterworth-Heinemann.

[14] Wei, Y., Barradas Berglind, J. D. J., Muhammad Zaki Almuzakki, M., van Rooij, M., Wang, R., Jayawardhana, B. & Vakis, A. I. 2018. *Proceedings of the 37th International Conference on Ocean, Offshore and Arctic Engineering*. ASME, 10 p.

Symbols

A	Area
a	Acceleration
c	Damping coefficient
D	Diameter
F_{ine}	Inertia Force
F_{gr}	Gravitational Force
F_{vis}	Viscosity Force
F_r	Froude Number
g	Gravitational constant
k	Spring Constant
k_{water}	Spring Constant Water Column
k_{down}	Spring Constant of the Water Column in Downstroke
k_{up}	Spring Constant of the Water Column in Upstroke
k_{rod}	Spring Constant of the Rod
L	Length
m	Mass
R_e	Reynolds Number
R_r	Rod Radius
SPP	Single Piston Pump
T	Time
V	Velocity

μ	Viscosity
ρ	Denisty
τ	Shear Stress
ω	Frequency

Appendix

Table of contents

Appendix A. Adjusted MATLAB-script [1:X]

```
%-------------------------------------------------------------------
% INITIATE DATA - CheckValveModelV3 _ Simulink model
% Model V 2.1
% Created by R.M. Zaharia
% Adjusted by J. Jonker
%-------------------------------------------------------------------
% if exist('read_data.m','file')
%     close all
% else
%     clear all
%     clc
%     close all
% end
%     clear all
%     close all
%     clc
%-------------------------------------------------------------------
% Ask for the values of the water level
%-------------------------------------------------------------------
    prompt = {'Initial level lower reservoir [m] :', ...
        'Initial level uppper reservoir [m]:','Motor arm setting:', ...
        'Motor frequency','Number of strokes:'};
    dlg_title = 'Initializiations';
    num_lines = 1;
    defaultans = {'1.197','1.658','7','15','3'};
    answer = inputdlg(prompt,dlg_title,[1 50],defaultans);

%-------------------------------------------------------------------
% Save the values in their own variable name
%-------------------------------------------------------------------
    for i = 1:size(answer)
        data(i) = str2num(answer{i});
    end

    init_low = data(1);
    init_up = data(2);
    motor_set = data(3);
    motor_freq = data(4);
    strokes = data(5);

%-------------------------------------------------------------------
% Switches and changeable parameters
%-------------------------------------------------------------------
    %X=5;
    global X;

    cv_amount = 12;                                % Number of ball valves
    pv_amount = 6;

%-------------------------------------------------------------------
% Simulation Parameter
%-------------------------------------------------------------------

    rho = 998.159;                        % [kg/m^3] Density of working fluid
    g = 9.81;                             % [m/s^2] Gravitational constant

%-------------------------------------------------------------------
% Motor Parameters
%-------------------------------------------------------------------
    m_setting = motor_set;
```

```
    f_setting = motor_freq;
    % Velocity of the motor based on the settings
    omega = (2*pi*(0.15+0.05*m_setting)/100)*f_setting;
    % amplitude
    amp = ((2*pi*(0.15+0.05*m_setting)^2)/100)*f_setting*sqrt(X);
    bias = 0;                                          % bias
    freq = omega*(1/sqrt(X));                                  % [rad/sec]
frequency
    phase = 0;                                         % [rad] Phase
    samp = 0;                                          % Sample time
    time = ((2*pi)/(abs(omega)))*strokes*sqrt(X); % [s] Running Time
    amp_m= 2*(0.15+0.05*m_setting)*X;
%-------------------------------------------------------------------------
% Reservoir Data
%-------------------------------------------------------------------------
    u_reservoir_width = 1.56*X;                    % [m] length of the reser-
voir
    u_reservoir_length = 1.97*X;                   % [m] width of the reser-
voir
    u_reservoir_height = 1*X;                      % [m] height of the reser-
voir
    init_height_u = init_up*X - 1.478*X;
    init_up_scaled = init_up*X;
    upper_reservoir_volume = init_height_u*u_reservoir_width*u_reser-
voir_length;
    % [m^3] Volume of the lower reservoir


    l_reservoir_width = 1.77*X;                    % [m] width of the reser-
voir
    l_reservoir_length = 2.27*X;                   % [m] length of the reser-
voir
    l_reservoir_height = 1*X;                      % [m] height of the reser-
voir
    init_height_l = init_low*X - 0.85*X;
    init_low_scaled = init_low*X;
    lower_reservoir_volume = init_height_l*l_reservoir_width*l_reser-
voir_length;
    % [m^3] Volume of the higher reservoir


    tank_cross_section_higher = u_reservoir_width * u_reservoir_length;

    tank_cross_section_lower = l_reservoir_width * l_reservoir_length;

    reservoir_pipe_diameter = 0.18*X;              % [m] Diameter of pipe
out and in reservoir

%-------------------------------------------------------------------------
% Pipe Data
%-------------------------------------------------------------------------
    % In this model, there are currently three pipes. The first from the
lower
    % reservoir to the check valve. The second from the check valve to the
    % piston. The third from the piston to the higher reservoir.

    % Materials
    % https://www.engineeringtoolbox.com/surface-roughness-ventilation-
ducts-d_209.html
```

```
    % https://www.researchgate.net/publication/230737556_Analysis_of_Sur-
face_Roughness_for_Laser_Cutting_on_Acrylic_Sheets_using_Response_Sur-
face_Method
    % http://www.scielo.br/scielo.php?script=sci_arttext&pid=S1415-
43662017000300143
    PVC = 0.0015e-3;                            % [m] Internal surface
roughness height
    metal = 0.015e-3;                           % [m] Internal surface
roughness height
    acryl = 5e-6;                               % [m] Internal surface
roughness height

    % Pipe (1) - material: PVC
    diameter_pipe_1 = 0.18*X;                     % [m] Diameter of the
first pipe
    height_A_1 = 0.6*X + 0.2;                           % [m] height of in-
let pipe wrt reference plane
    height_B_1 = 0.2;                           % [m] height of inlet pipe
wrt reference plane
    pipe_length_1 = height_A_1 - height_B_1;    % [m] Lenght of the first
pipe


if piping_choice > 0
    % Bend (2) - material: PVC
    diameter_pipe_2 = 0.18*X;                     % [m] Diameter of bend
    area_pipe_2 = pi*(diameter_pipe_2/2)^2;
    bend_radius_2 = 0.3*X;                        % [m] Bend radius
    bend_angle_2 = 90;                          % [degrees] Bend angle

    % Pipe (3) - material: PVC
    diameter_pipe_3 = 0.18*X;
    pipe_length_3 = 1.41*X;
    height_A_3 = 0.2;
    height_B_3 = 0.2;

    % Butterfly Valve (4) - material: PVC
    length_pipe_4 = 0.2*X;
    diameter_valve_4 = 0.16*X;
    area_valve_4 = pi*(diameter_valve_4/2)^2;
    flow_discharge_4 = 0.856*X^(5/2);

    % Pipe (5) - material: PVC
    diameter_pipe_5 = 0.18*X;
    pipe_length_5 = 0.94*X;
    height_A_5 = 0.2;
    height_B_5 = 0.2;

    % Bend (6) - material: PVC
    diameter_pipe_6 = 0.18*X;                     % [m] Diameter of bend
    bend_radius_6 = 0.18*X;                       % [m] Bend radius
    bend_angle_6 = 90;                          % [degrees] Bend angle
    area_pipe_6 = pi*(diameter_pipe_6/2)^2;     % [m^2] surface area

    % Pipe (7) - material: PVC
    diameter_pipe_7 = 0.18*X;
    pipe_length_7 = 0.175*X;
    height_A_7 = 0.2;
    height_B_7 = 0.2;

    % Butterfly Valve (8) - material: PVC
```

```
    diameter_valve_8 = 0.16*X;
    flow_discharge_8 = 0.856*X^(5/2);

    % Pipe (9) - material: PVC
    diameter_pipe_9 = 0.18*X;
    pipe_length_9 = 0.755*X;
    height_A_9 = 0.2;
    height_B_9 = 0.2;

    % Bend (10) - material: PVC
    diameter_pipe_10 = 0.18*X;                      % [m] Diameter of bend
    bend_radius_10 = 0.3*X;                         % [m] Bend radius
    bend_angle_10 = 90;                            % [degrees] Bend angle
    area_pipe_10 = pi*(diameter_pipe_10/2)^2;      % [m^2] surface area
else
% ------------ SMALL PIPING PARAMETERS ARE FOUND HERE!!!! -----------------
    % Bend (2) - material: PVC
    diameter_pipe_2 = 0.10*X;                       % [m] Diameter of bend
    area_pipe_2 = pi*(diameter_pipe_2/2)^2;
    bend_radius_2 = 0.1*X;                          % [m] Bend radius
    bend_angle_2 = 90;                             % [degrees] Bend angle

    % Pipe (3) - material: PVC
    diameter_pipe_3 = 0.10*X;
    pipe_length_3 = 1.41*X;
    height_A_3 = 0.2;
    height_B_3 = 0.2;

    % Butterfly Valve (4) - material: PVC
    length_pipe_4 = 0.2*X;
    diameter_valve_4 = 0.10*X;
    area_valve_4 = pi*(diameter_valve_4/2)^2;
    flow_discharge_4 = 0.856*(X^(5/2));

    % Pipe (5) - material: PVC
    diameter_pipe_5 = 0.10*X;
    pipe_length_5 = 0.94*X;
    height_A_5 = 0.2;
    height_B_5 = 0.2;

    % Bend (6) - material: PVC
    diameter_pipe_6 = 0.10*X;                       % [m] Diameter of bend
    bend_radius_6 = 0.18*X;                         % [m] Bend radius
    bend_angle_6 = 90;                             % [degrees] Bend angle
    area_pipe_6 = pi*(diameter_pipe_6/2)^2;        % [m^2] surface area

    % Pipe (7) - material: PVC
    diameter_pipe_7 = 0.10*X;
    pipe_length_7 = 0.175*X;
    height_A_7 = 0.2;
    height_B_7 = 0.2;

    % Butterfly Valve (8) - material: PVC
    diameter_valve_8 = 0.16*X;
    flow_discharge_8 = 0.856*(X^(5/2));

    % Pipe (9) - material: PVC
    diameter_pipe_9 = 0.10*X;
    pipe_length_9 = 0.755*X;
    height_A_9 = 0.2;
    height_B_9 = 0.2;
```

```
    % Bend (10) - material: PVC
    diameter_pipe_10 = 0.10*X;                          % [m] Diameter of bend
    bend_radius_10 = 0.1*X;                             % [m] Bend radius
    bend_angle_10 = 90;                                % [degrees] Bend angle
    area_pipe_10 = pi*(diameter_pipe_10/2)^2;          % [m^2] surface area
end
% ------------- END SMALL PIPING PARAMETERS -----------------------------
    % Pipe (11) - material: PVC
    diameter_pipe_11 = 0.18*X;
    height_A_11 = 0.2;
    height_B_11 = 0.66*X + 0.2;
    pipe_length_11 = height_B_11 - height_A_11;


    % Pipe (12) CV - material: PVC
    diameter_pipe_12 = 0.18*X;
    height_A_12 = 0.5*X + 0.2;
    height_B_12 = 0.8*X +0.2;
    pipe_length_12 = height_B_12 - height_A_12;


    % Pipe (13) - material: PVC
    diameter_pipe_13 = 0.18*X;
    height_A_13 = 1.34*X +0.2;
    height_B_13 = 2.15*X +0.2;
    pipe_length_13 = height_B_13 - height_A_13;


    % Pipe (14) - material: PVC
%     diameter_pipe_14 = 2;
%     pipe_length_14 = 50;
%     height_A_14 = 3.95;
%     height_B_14 = 53.95;

    diameter_pipe_14 = 0.18*X;
    pipe_length_14 = 0.01*X;
    height_A_14 = 3.75*X + 0.2;
    height_B_14 = 3.76*X + 0.2;


    % Pipe (14) - material: Metal - Piston Cylinder
    % See other section

%-------------------------------------------------------------------------
% Check Valve Data
%-------------------------------------------------------------------------
     r_cv = 0.02*X;                          % [m] Radius passage area Check
Valve
     max_passage_area_cv = pi*(r_cv)^2;% [m^2] Maximum passage area Check
Valve
     crack_cv = 1e1*X;                                % [Pa] Cracking Pressure
CV
     max_cv = 1e4*X;                                   % [Pa] Maximum opening
pressure CV
     leak_cv = 1e-10;                                 % [m^2] Leakage area
     opening_cv = 0.1;                               % [s] Opening time con-
stant
     init_area_cv = 1e-10;                            % [m^2] initial area CV

    % Piping before and after the check valve
```

```
    cv_up_pipe_l = 0.3175*X;                          % [m] upper pipe cv
    cv_up_A = 1.04*X+0.2;
    cv_up_B = 1.34*X+0.2;
    r_pipe_up = 0.18*X;                             % [m] diameter upper cv
pipe
    cv_down_pipe_l = 0.3175*X;                        % [m] down pipe cv
    cv_down_A = 0.66*X+0.2;
    cv_down_B = 0.97*X+0.2;
    r_pipe_down = 0.18*X;                           % [m] diameter down cv
pipe

    % Fluid inertia should also be taken into account for the CV (see block
    % there).
    height_cv = 0.035*X;                            % [m] height of the CV
%-------------------------------------------------------------------
% Piston Pump Parameters (without Valve)
%-------------------------------------------------------------------
    mass = 25*X^3;                                    % [kg] Mass piston/rod
    Rr = 0.0025;                                    % [m] Radius rod
    Est = 210e9;                                    % Young's Modulus of steel
    Lr = 5*X;                                         % [m] Length rod
    zeta = 25;                                      % Rod damping ratio
    K1 = (pi*(Rr^2)*Est)/Lr;
    C1 = 2*zeta*sqrt(mass*K1);
%     K2 = rho*g*(pi*(0.09)^2);

    l_pipe_t = pipe_length_1 + pipe_length_3 + pipe_length_5 + ...
        pipe_length_7 + pipe_length_9 + pipe_length_11 + pipe_length_12 ...
        + pipe_length_13 + 4;
    m_pipes = pi * (0.09^2) * l_pipe_t * rho;

    n_freq = sqrt((2*g)/l_pipe_t);
    c_ratio = 0.098;
    % Damping water column
    C2 = 2*0.5*m_pipes*n_freq*c_ratio;

    % Stiffness
    K2 = 2*rho*(pi*0.095^2)*g;

%     damper = (C1 + C2)/300;
%     spring = (1/((1/K1)+(1/K2)))*300  ;


    piston_rad = 0.089*X;                             % [m] Radius of piston
    piston_area = pi*piston_rad^2;                  % [m^2] Piston area
    pipe_piston_l = 1.6*X;                            % length piston cylin-
der
    pipe_piston_d = 0.20*X;
    pipe_piston_A = 2.15*X+0.2;
    pipe_piston_B = 3.75*X+0.2;

%-------------------------------------------------------------------
% Valve in Piston Parameters (pv = piston valve)
%-------------------------------------------------------------------
%     total_area_pv = pi*0.05^2;
%     max_passage_area_pv = total_area_pv/6;
    r_pv = 0.01*X;                                    % [m] Radius passage
area Check Valve
    max_passage_area_pv = pi*(r_pv)^2;              % [m^2] Maximum passage
area Check Valve
```

```
    crack_pv = 0.1e1*X;                                 % [Pa] Cracking Pres-
sure CV
    max_pv = 2.2e4*X;                                   % [Pa] Maximum opening
pressure CV
    leak_pv = 1e-10;                                  % [m^2] Leakage area
    opening_pv = 0.1;                                 % [s] Opening time con-
stant
    init_area_pv = 1e-10;                             % [m^2] initial area CV

    piston_height = 0.3*X;

     % Vertical piping section 1
    l_section_1 = pipe_length_1 + bend_radius_2;
    % Vertical piping section 2
    l_section_2 = bend_radius_10 + pipe_length_11 + cv_down_pipe_l + ...
        cv_up_pipe_l + height_cv + pipe_length_13 + pipe_piston_l + ...
        pipe_length_14;

%-------------------------------------------------------------------------
% Fluid Properties
%-------------------------------------------------------------------------
    temp = 18;                                      % [deg Celcius] Temperature
    % Density, viscosity and bulk modulus depends on settings, but with 18
    % degrees it is as follows:
    % density (kg/m^3) = 998.159
    % Viscosity (cST): 1.05678
    % Bulk Modulus (Pa): 2.16651e+09
    T = 13.33*sqrt(X);                             %period
    %init_mass= rho * g * (h_head_sim - init_low_scaled) * piston_area;
```

Appendix B. Adjusted Calculation MATLAB-script

```
%-------------------------------------------------------------------------
% Calculations
% Created by R.M. Zaharia
% Adjusted by J. Jonker
%-------------------------------------------------------------------------

% Hydraulic head [m] - difference between both bottom reservoirs

for k = 1:size(tout)
    delta_h(k) = l_upper_reservoir(k) + l_section_2 - l_lower_reservoir(k)
- ...
        l_section_1;
end


%Take only the force in the upstroke
    forceUp = zeros(size(tout));
    for i = 1:size(tout),
        if motor_force1(i) > 0
            forceUp(i) = motor_force1(i);
        else
            forceUp(i) = 0;
        end
    end

 % determining the amount of water pumped up
    pumped_upper_sim = volume_up(end)-volume_up(1);
    pumped_lower_sim = volume_down(end) - volume_down(1);
    avg_pumped_sim = (pumped_upper_sim - pumped_lower_sim)/2;
    pumped_int_sim = avg_pumped_sim/length(tout);
```

```
    pumped_total_sim = sum(net_flow(600:end))./(size(tout)./time);


% Calculating the potential energy
    Epot = zeros(length(tout),1);
    Ppot_sim = zeros(size(tout));
    h_head_sim = zeros(size(tout));

for i = 1:size(tout),
    h_head_sim_end = delta_h(end);
    h_head_sim(i) = delta_h(i);
    Epot(i) = rho*g*(sum(h_head_sim)/length(tout))*pumped_int_sim;

    Ppot_sim(i) = rho*g*h_head_sim(i);
end

    Epot1 = Epot;
    Epot = sum(Epot);

    avg_pumped_sim = abs(volume_up(end) - volume_up(1));
    max_pumped_sim = max(position_motor)*(pi*piston_rad^2)*(strokes);
    vol_efficiency_sim = (avg_pumped_sim/max_pumped_sim)*100;

    Ppump_sim = piston_velocity .* motor_force1;
    Ppot_end = rho*g*delta_h(end);
    Epump = trapz(tout,Ppump_sim);

    tot_eff = Epot / Epump * 100;
    mec_eff = tot_eff / vol_efficiency_sim * 100;

    init_mass= rho * g * (delta_h) * piston_area;
    init_mass_transposed= init_mass.';
    piston_force_normalized = (motor_force1) ./ (init_mass_transposed);
    piston_pos_amp = position_motor / amp_m;
    % Print Results
if disp_data > 0

        disp(['------------------------------------------------------------
']);
        disp(['|          Results Simulink Model          |']);
        disp(['--------------------------']);
        disp(['Average Max displacement = ',num2str(max(position_motor)),'
m']);
    %     disp(['Average Wave Period = ',num2str(mean(Aperiod)),' Sec']);
    %     disp(['Upper level start = ',num2str(mean(h_upper_start)),' m']);
    %     disp(['Lower level start = ',num2str(mean(h_lower_start)),' m']);
        disp(['--------------------------']);
        disp(['Total Pumping energy = ',num2str(Epump),' J']);
        disp(['Total Potential energy = ',num2str(Epot),' J']);
        disp(['Avg. Pumping energy per stroke = ',num2str(Epump/strokes),'
J']);
        disp(['Avg. Potential energy per stroke = ',num2str(Epot/strokes),'
J']);
        disp(['--------------------------']);
        disp(['Volumetric Efficiency = ',num2str(vol_efficiency_sim),'
%']);
        disp(['Mechanical Efficiency = ',num2str(mec_eff),' %']);
        disp(['Total Efficiency = ',num2str(tot_eff),' %']);
else
    disp(['Nothing to show here'])
end
```

Appendix C. Adjusted Run Simulink model

```
%-------------------------------------------------------------------------
% Run model - CheckValveModelV5 _ Simulink model
% Model V 3.0
% Created by R.M. Zaharia
% Adjusted by J. Jonker
%-------------------------------------------------------------------------

    clearvars -except X x_solution y_solution index;

 %% Unnecessary code
%           clear all
%           clc
%           close all
%
% Switches
    calculations_data   = 1;    % Run the calculations
    display_data        = 1;    % Display the data
    plot_results        = 0;    % Plot results (see plot file)
    piping_choice       = 1;    % 1 is large piping, 0 is small piping

%-------------------------------------------------------------------------
% Run the simulation
%-------------------------------------------------------------------------
initialization_parametersV5
    global X;
    damper = 43000*X^2;                         % [N/m] Damper
    spring = 1*X^2;                                % [N/m] Spring

    % Run the simulink model
    disp('Simulation is running...');
    options = simset('SrcWorkspace','current');
    sim('checkValveModelV5',[],options);

%-------------------------------------------------------------------------
% Determine the switches
%-------------------------------------------------------------------------
if calculations_data > 0
    if display_data > 0
        disp_data = 1;
    else
        disp_data = 0;
    end
calculationsSimulinkV4
end

if plot_results > 0
    plot_simulinkresults
end
```

Appendix D. MATLAB-scripts to Plot

Piston Force

```
global X;

%% run scripts
for index = 1:4
    X = index ;
    run_simulinkmodelV4;
```

```
    x_solution{index} = tout/T;
    y_solution{index} = piston_force_normalized;
end

%% Plot solutions
cmap = {'r', 'g', 'b', 'k', 'c', 'm', 'y'};
figure('visible', 'off');
for index = 1:4
    plot(x_solution{index}, y_solution{index}, 'Color', cmap{index});
    leg{index} = (strcat('Lr = ', num2str(index )));
    hold on;
end
legend(leg);
title("Piston Force normalized with [1:X] scaling ");
xlabel('time/period');
ylabel('Force/mass');
saveas(gcf, 'piston_force_normalized.png');
```

Piston displacement divided by motor amplitude

```
global X;

%% run scripts
for index = 1:4
    X = index;
    run_simulinkmodelV4;
    x_solution{index} = tout/T;
    y_solution{index} = piston_pos_amp;
end

%% Plot solutions
cmap = {'r', 'g', 'b', 'k', 'c', 'm', 'y'};
figure('visible', 'off');
for index = 1:4
    plot(x_solution{index}, y_solution{index}, 'Color', cmap{index});
    leg{index} = (strcat('Lr = ', num2str(index)));
    hold on;
end
legend(leg);
title("Piston Displacement normalized with [1:X] scaling ");
xlabel('time/period');
ylabel('Position');
saveas(gcf, 'piston_pos_amp.png');
```

Potential energy

```
global X;

%% run scripts
for index = 1:4
    X = index;
    run_simulinkmodelV4;
    x_solution(index) = X;
    y_solution(index) = Epot;
end

%% Plot solutions
%cmap = {'r', 'g', 'b', 'k', 'c', 'm', 'y'};
figure('visible', 'off');
for index = 1:4
    %plot(x_solution[array], y_solution[array], 'Color', cmap{index});
    %plot(X, y_solution(index));
    plot(x_solution , y_solution);
```

```
    %leg{index} = (strcat('Lr = ', num2str(index * 0.5 + 0.5)));
    %hold on;
end
% %legend(Epot);

title("Potential Energy with [1:X] scaling");
 xlabel('Scaling (Lr)');
 ylabel('Energy (J)');
 saveas(gcf, 'epot.png');
```

Flow through the check valve

```
global X;

%% run scripts
for index =1:3
    X = index+2;
    run_simulinkmodelV4;
    x_solution{index} = tout/T;
    y_solution{index} = flow_cv_total;
end

%% Plot solutions
cmap = {'r', 'g', 'b', 'k', 'c', 'm', 'y'};
figure('visible', 'off');
for index = 1:3
    plot(x_solution{index}, y_solution{index}, 'Color', cmap{index});
    leg{index} = (strcat('Lr = ', num2str(index+2)));
    hold on;
end
legend(leg);
title("");
xlabel('time/period');
ylabel('\Delta P [Pa]');
saveas(gcf, 'flowCV_16.png');
```

Appendix F. Initial Parameters

Motor parameter	Parameter	Value	Dimension	Description	Froude Scaling
	m_setting	motor_set	-		
	f_setting	motor_freq	-		
	omega	(2*pi*(0.15+0.05*m_setting)/100)*f_setting	m		
	amp	((2*pi*(0.15+0.05*m_setting)^2)/100)*f_setting	m		Sqrt(X)
	bias	0			
	freq	omega	H		1/sqrt(X)
	phase	0	-		

	samp	0	-		
	time	((2*pi)/(abs(omega)))* strokes	s		sqrt(X)

Resevoir data	Parameter	Value	Di-men-sion	Description	Froude Sca-ling
	u_re-sevoir_width	1.56	m	Width of upper reservoir	X
	u_re-sevoir_length	1.97	m	Length of upper reservoir	X
	u_re-sevoir_height	1	m	Height of upper reservoir	X
	init_height_u	init_up - 1.478	m	Initial height of upper reservoir	X
	upper_re-sevoir_vo-lume	init_height_u*u_re-sevoir_width*u_re-sevoir_length	m^3	Volume of upper reservoir	X^3
	l_re-sevoir_width	1.77	m	Width of lower reservoir	X
	l_re-sevoir_length	2.27	m	Length of lower reservoir	X
	l_re-sevoir_height	1	m	Height of lower reservoir	X
	init_height_l	init_low - 0.85	m	Initial height of lower reservoir	?
	lower_re-sevoir_vo-lume	init_height_l*l_rese-voir_width*l_rese-voir_length	m^3	Volume of lower reservoir	X^3
	tank_cross_sec-tion_hig-her	u_resevoir_width * u_resevoir_length	m^2	Cross section of upper reservoir	X^2

	tank_cross_section_lower	l_resevoir_width * l_resevoir_length	m^2	Cross section of lower reservoir	X^2
	resevoir_pipe_diameter	0.18	m	Diameter of pipe in and out the reservoir	X

	Parameter	Value	Dimension	Description	Froude Scaling
Pipe data	PVC	0.0015e-3	m	Internal surface roughness height	
	Metal	0.015e-3	m	Internal surface roughness height	
	Acryl	5,00E-06	m	Internal surface roughness height	
Pipe (1) - material: PVC	diameter_pipe_1	0.18	m	Diameter of pipe 1	X
	height_A_1	0.8	m	Height of inlet pipe wrt reference plane	X
	height_B_1	0.2	m	Height of outlet pipe wrt reference plane	X
	pipe_length_1	height_A_1 - height_B_1	m	Length of the first pipe	X
if piping choice > 0					
Bend (2) - material: PVC	diameter_pipe_2	0.18	m	Diameter of bend 2	X
	area_pipe_2	pi*(diameter_pipe_2/2)^2	m^2	Area of pipe 2	X^2
	bend_radius_2	0.3	m	Bend radius of pipe 2	X
	bend_angle_2	90	degrees	Bend angle of pipe 2	
Pipe (3)	diameter_pipe_3	0.18	m	Diameter of pipe 3	X
	pipe_length_3	1.41	m	Lenght of pipe 3	X

	height_A_3	0.2	m	Height of inlet wrt reference plane	X
	height_B_3	0.2	m	Height of inlet wrt reference plane	X
Butterfly Valve (4) - material: PVC	diame-ter_pipe_4	0.16	m	Diameter of pipe 4	X
	area_valve_4	pi*(diame-ter_valve_4/2)^2	m^2	Area of valve 4	X^2
	length_pipe_4	0.2	m	Length of pipe 4	x
	flow_discharge_4	0.856	m^3/s	Flow discharge of valve 4	X^(5/2)
Pipe (5) - material: PVC	diame-ter_pipe_5	0.18	m	Diameter of pipe 5	X
	pipe_length_5	0.94	m	Lenght of pipe 5	X
	height_A_5	0.2	m	Height of inlet wrt reference plane	X
	height_B_8	0.2	m	Height of outlet wrt reference plane	X
Bend (6) - material: PVC	diame-ter_pipe_6	0.18	m	Diameter of pipe 6	X
	area_pipe_6	pi*(diame-ter_pipe_6/2)^2	m^2	Area of pipe 6	X^2
	bend_ra-dius_6	0.18	m	Bend radius of pipe 6	X
	bend_an-gle_6	90	m	Bend angle of pipe 6	X
Pipe (7)	diame-ter_pipe_7	0.18	m	Diameter of pipe 7	X
	pipe_length_7	0.175	m	Length of pipe 7	X
	height_A_7	0.2	m	Height of inlet wrt reference plane	X
	height_B_7	0.2	m	Height of outlet wrt reference plane	X

Butterfly Valve (8) - material: PVC	diameter_valve_8	0.16	m	Diameter of valve 8	X
	flow_discharge_8	0.856	m^3/s	Flow discharge of valve 4	X^(5/2)
Pipe (9)	diameter_pipe_9	0.18	m	Diameter of pipe 9	X
	length_pipe_9	0.775	m	Lenght of pipe 9	X
	height_A_9	0.2	m	Height of inlet wrt reference plane	X
	height_B_9	0.2	m	Height of inlet wrt reference plane	X
Bend (10) - material: PVC	diameter_pipe_10	0.18	m	Diameter of pipe 10	X
	area_pipe_10	pi*(diameter_pipe_10/2)^2	m^2	Area op pipe 10	X^2
	bend_radius_10	0.3	m	Bend radius of pipe 10	X
	bend_angle_10	90	m	Bend angle of pipe 10	X
else (small piping parameters)					
Bend (2) - material: PVC	diameter_pipe_2	0.10	m	Diameter of bend 2	X
	area_pipe_2	pi*(diameter_pipe_2/2)^2	m^2	Area of pipe 2	X
	bend_radius_2	0.1	m	Bend radius of pipe 2	X
	bend_angle_2	90	degrees	Bend angle of pipe 2	X
Pipe (3)	diameter_pipe_3	0.10	m	Diameter of pipe 3	X
	pipe_length_3	1.41	m	Length of pipe 3	X
	height_A_3	0.2	m	Height of inlet wrt reference plane	X

	height_B_3	0.2	m	Height of outlet wrt reference plane	X
Butterfly Valve (4) - material: PVC	diame-ter_valve_4	0.10	m	Diameter of pipe 4	X
	area_valve_4	pi*(diame-ter_valve_4/2)^2	m^2	Area of valve 4	X^2
	length_pipe_4	0.2	m	Length of pipe 4	X
	flow_discharge_4	0.856	m^3/s	Flow discharge of valve 4	X^(5/2)
Pipe (5) - material: PVC	diame-ter_pipe_5	0.10	m	Diameter of pipe 5	X
	pipe_length_5	0.94	m	Lenght of pipe 5	X
	height_A_5	0.2	m	Height of inlet pipe wrt reference plane	X
	height_B_8	0.2	m	Height of outlet pipe wrt reference plane	X
Bend (6) - material: PVC	diame-ter_pipe_6	0.1	m	Diameter of pipe 6	X
	area_pipe_6	pi*(diame-ter_pipe_6/2)^2	m^2	Area of pipe 6	X^2
	bend_ra-dius_6	0.18	m	Bend radius of pipe 6	X
	bend_an-gle_6	90	m	Bend angle of pipe 6	X
Pipe (7)	diame-ter_pipe_7	0.10	m	Diameter of pipe 7	X
	pipe_length_7	0.175	m	Length of pipe 7	X
	height_A_7	0.2	m	Height of inlet pipe wrt reference plane	X
	height_B_7	0.2	m	Height of outlet pipe wrt reference plane	X

Butterfly Valve (8) - material: PVC	diameter_valve_8	0.16	m	Diameter of valve 8	X
	flow_discharge_8	0.856	m^3/s	Flow discharge of valve 4	X^(5/2)
Pipe (9)	diameter_pipe_9	0.10	m	Diameter of pipe 9	X
	pipe_length_9	0.755	m	Length of pipe 9	X
	height_A_9	0.2	m	Height of inlet pipe wrt reference plane	X
	height_B_9	0.2	m	Height of outlet pipe wrt reference plane	X
Bend (10) - material: PVC	diameter_pipe_10	0.1	m	Diameter of pipe 10	X
	area_pipe_10	pi*(diameter_pipe_10/2)^2	m^2	Area op pipe 10	X^2
	bend_radius_10	0.1	m	Bend radius of pipe 10	X
	bend_angle_10	90	m	Bend angle of pipe 10	X
End small piping					
Pipe (11) - material: PVC	diameter_pipe_11	0.18		Diameter of pipe 11	X
	height_A_11	0.2	m	Height of inlet pipe wrt reference plane	X
	height_B_11	0.86	m	Height of outlet pipe wrt reference plane	X
	pipe_length_11	height_B_11 - height_A_11	m	Length of pipe 11	X
Pipe (12) - material: PVC	diameter_pipe_12	0.18	m	Diameter of pipe 12	X

	height_A_12	0.7	m	Height of inlet pipe wrt reference plane	X
	height_B_12	1	m	Height of outlet pipe wrt reference plane	X
	pipe_length_12	height_B_12 - height_A_12	m	Length of pipe 12	X
Pipe (13) - material: PVC	diameter_pipe_13	0.18	m	Diameter of pipe 13	X
	height_A_13	1.54	m	Height of inlet pipe wrt reference plane	X
	height_B_13	2.35	m	Height of outlet pipe wrt reference plane	X
	pipe_length_13	height_B_13 - height_A_13	m	Length of pipe 13	X
Pipe (14) - material: PVC	diameter_pipe_14	0.18	m	Diameter of pipe 14	X
	height_A_14	3.95	m	Height of inlet pipe wrt reference plane	X
	height_B_14	3.96	m	Height of outlet pipe wrt reference plane	X
	pipe_length_14	0.01	m	Length of pipe 14	X

Check Valve Data	Parameter	Value	Dimension	Description	Froude Scaling
	r_cv	0.02	m	Radius passage area check valve	X
	max_passage_area_cv	pi*(r_cv)^2	m^2	Maximum passage area check valve	X^2
	crack_cv	1,00E+01	Pa	Cracking pressure CV	X
	max_cv	1,00E+04	Pa	Maximum opening pressure CV	X

	leak_cv	1,00E-10	m^2	Leakage area	X^2
	opening_cv	0.1	s	Opening time constant	
	init_area_cv	1,00E-10	m^2	initial area CV	X^2
	Piping before and after the check valve				
	cv_up_pipe_1	0.3175	m	upper pipe cv	X
	cv_up_A	1.24	m		X
	cv_up_B	1.54	m		X
	r_pipe_up	0.18	m	diameter upper cv pipe	X
	cv_down_pipe_1	0.3175	m	down pipe cv	X
	cv_down_A	0.86	m		X
	cv_down_B	1.17	m		X
	r_pipe_down	0.18	m	diameter down cv pipe	X
	height_cv	0.035	m	height of the cv	X

Piston pump parameters (without valve)	Parameter	Value	Dimension	Description	Froude Scaling
	mass	25	kg	Q^3	X^3
	Rr	0.0025	m		X
	Est	2,10E+11	Young modulus of steel		
	Lr	5	m		X
	zeta	25	rod damping ratio		
	K1	(pi*(Rr^2)*Est)/Lr	-	-	-
	C1	2*zeta*sqrt(mass*K1)	-	-	-
	%K2	rho*g*(pi*(0.09)^2)	-	-	-
	l_pipe_t	pipe_length_1 + pipe_length_2 + ..+pipe_length 14	m		X

	m_pipes	pi * (0.09^2) * l_pipe_t * rho	m^3		X^3
	n_freq	sqrt((2*g)/l_pipe_t)	-	-	-
	c_ratio	0.098	-	-	-
	Damping water column				
	C2	2 * 0.5 * m_pipes * n_freq * c_ratio	-	-	-
	Stiffness				
	K2	2 * rho * (pi * 0.095^2) * g	-	-	-
	%damper	(C1 + C2)/300	-	-	-
	%spring	(1/((1/K1) + (1/K2))) * 300	-	-	-
	piston_rad	0.089	m	Radius of piston	X
	piston_area	pi * piston_rad^2	m^2	Piston area	X^2
	pipe_piston_l	1.6	m	length piston cylinder	X
	pipe_piston_d	0.20	m		X
	pipe_piston_A	2.35	m		X
	pipe_piston_B	3.95	m		X

Valve in Piston parameters	Parameter	Value	Dimension	Description	Froude Scaling
	r_pv	0.01	m	Radius passage area	X

				check valve	
	max_passage_area_pv	pi*(r_pv)^2	m^2	Maximum passage area check valve	X^2
	crack_pv	0.1e1	Pa	cracking pressure CV	X
	max_pv	2.2e4	Pa	maximum opening pressure CV	X
	leak_pv	1,00E-10	m^2	Leakage area	X
	opening_pv	0.1	s	opening time constant	
	init_area_pv	1,00E-10	m^2	initial area CV	X^2
	piston height	0.3	m	Height of the piston	X
	Vertical piping section 1				
	l_section_1	pipe_length_1 + bend_radius_2	m	Length of section 1	X
	Vertical piping section 2				
	l_section_2	bend_radius_10 + pipe_length_11 + cv_down_pipe_l + cv_up_pipe_l + height_cv + pipe_length_13 + pipe_piston_l + pipe_length_14	m	Length of section 2	X